Chapter 4
Shelf Dynamics and Transient Coastal Upwelling: Data Observations

4.1 INTRODUCTION

Hydrodynamics play a key role in regulating shelf phytoplankton abundances through their role as an implicit controller of nutrient supply and exchange in shelf waters. In the waters surrounding New Zealand, shelf dynamics may be forced by a variety of mechanisms, from the relatively short time-scales associated with tides and meteorological events, to longer term variations in oceanic flows (Sharples and Greig, 1998). Shelf dynamics leading to coastal upwelling provide an efficient mechanism to support primary production through sustained or periodic inputs of new nutrients.

The environmental and ecological sustainability of aquaculture developments within the Bay of Plenty is dependant on a balance between the scale of aquaculture and the productive and assimilative capacity of the shelf environment. Advanced knowledge of shelf physical dynamics, including forcings, interactions, and associated response mechanisms is an essential precursor to understanding ecosystem processes driving primary production on the shelf.

4.2 MOTIVATION AND RELEVANCE TO THESIS OBJECTIVES

The present lack of research and understanding of the physical dynamics of the Bay of Plenty shelf environment hinders informed decision making regarding the development of a sustainable aquaculture industry. Relatively few oceanographic investigations have been focussed within the study area, though this is not unusual for New Zealand coastal waters (de Lange *et al.*, 2003). There is no information on, or knowledge of, the detailed workings of specific forcing mechanisms, interactions and the associated dynamic responses within the Bay of Plenty.

The Bay of Plenty shelf morphology is such that over length scales of ~150 km the general shelf orientation changes by ~90^{o} and the general coast line orientation changes by ~ 135^{o} (Figure 2.3). Additionally, the variation in shelf and coastal orientation over length scales of ~50 km leads to variation in shelf widths over similar scales, creating potentially complex physical dynamics. The region is a site of potential offshore aquaculture developments and an understanding of physical dynamic processes and nutrient delivery mechanisms is vital for the efficient planning and management of the industry. Several studies have established remarkably strong direct links (R^2=0.77) between upwelling indices and cultured shellfish production

and quality (Blanton *et al.*, 1987; Figueiras *et al.*, 2002). Furthermore, given that certain levels of current speeds can help prevent bio-deposit build up through enhanced waste dispersal and also promote the exchange and replacement of water within an aquaculture site (Hartstein and Rowden, 2004; Pillay, 2004; Perez *et al.*, 2005), advanced knowledge of the hydrodynamic environment significantly aids planning.

4.2.1 CHAPTER AIMS

This chapter aims to characterise the hydrodynamic environment and also to resolve the influence of wind forcing on the Bay of Plenty shelf environment using measured data. The focus is on:

- detailing the shelf environment with respect to
    - density stratification;
    - tidal currents;
    - residual circulation;
    - nutrient delivery;
- identification of the influence on circulation and characteristic response to wind-forcing; and the
- provision of essential data for the calibration and validation of both hydrodynamic and primary production numerical models.

4.3 BACKGROUND: WIND INDUCED UPWELLING

Coastal upwelling supports approximately half the world's captured fish production (Kampf *et al.*, 2004). Major coastal upwelling zones (*e.g.* Peruvian, Benguela, North African) are generally located at the eastern margins of subtropical ocean gyres, and driven predominantly by wind dynamics (*e.g.* Pickard and Emery, 1990; Mann and Lazier 1996). On western oceanic boundaries, however, the mean wind field is generally not conducive to persistent upwelling. Nonetheless, transient upwelling favourable wind stresses persisting beyond a diurnal cycle have been observed to lead to episodic coastal upwelling (Garvine, 1971, Smith, 1981). Such events have been observed on the southeastern and eastern U.S. continental shelf (*e.g.* Paffenhofer *et al.*, 1987; Yankovsky, 2003), the southern and eastern coasts of Australia (*e.g.* McClean-Padman and Padman, 1991; Lee *et al.*, 2001; Kampf *et al.*, 2004).

The established pattern of simplified wind-driven coastal upwelling can be described by stress balances, Ekman dynamics and pressure gradients (*e.g.* Csanady, 1981 and 1982; Pond and Pickard, 1983). Along-shelf wind stresses generate offshore Ekman transport of surface waters. Divergence of Ekman transport near the coast sets up a cross-shelf pressure gradient which in turn leads to an along-shelf geostrophic coastal current in the same direction as the wind stress. This along-shelf geostrophic current

accelerates until the bottom stress balances the wind stress, which occurs over a frictional time scale, t_f (Csanady, 1981; Smith, 1981). Onshore flows occur initially through the interior of the water column ($t < t_f$), as the surface layer is peeled off by the wind stress (Csanady, 1982; Dever, 1997), and then through the bottom Ekman layer ($t > t_f$). The initial interior onshore transport results from a balance between inertia (the accelerating along-shelf jet) and the Coriolis force (Allen *et al.*, 1995; Huthnance, 1995; Yankovsky, 2003).

Within New Zealand, wind forced Ekman upwelling and downwelling has previously been observed within the outer Hauraki Gulf (Sharples, 1997; Sharples and Greig, 1998; Zeldis *et al.*, 2004a). Modelling efforts within the Hauraki Gulf have also highlighted the response of shelf circulation to wind stresses (Proctor and Greig, 1989; Black *et al.*, 2000). No similar observations or modelling efforts have thus far been made within the Bay of Plenty.

In addition to forcing from wind stresses, upwelling has been observed as a result of persistent along-shelf flow at the shelf break (Hsueh and O'Brien, 1971; Oke and Middleton, 2000), cross-shelf transport associated with coastal trapped waves, longshore topographic variability (Rochford, 1975; Crèpon *et al.*, 1984; Roughan and Middleton, 2002), tidally induced currents, and the encroachment of large scale oceanic eddies onto the shelf (McClean-Padman and Padman, 1981).

4.4 DATA SOURCES AND SAMPLING METHODOLOGY

For the purposes of this study, dedicated research voyages were undertaken to gather oceanographic datasets and deploy long-term current meter / thermistor moorings. SST and Chlorophyll-a (Chl-a) retrievals were performed on remotely sensed datasets.

Physical sampling within the Bay of Plenty occurred between October 2003 and August 2004 over six campaigns. Sampling was concentrated along three transects extending from the nearshore (10 m depth) to the shelf edge (200 m depth), at Pukehina, Whakatane and Opotiki (Figure 4.1). Mooring deployments (*e.g.* PUK65 and OPO65 sites) along with more spatially dense short term sampling surveys were undertaken from the *MV Macy Gray* and *Port Whakatane II*. Each voyage included systematic Conductivity Temperature Density (CTD) profiling at 10, 20, 30, 50, 100, and 200 m depth contours along each transect, ensuring neritic coastal waters were covered with enough resolution while also allowing comparison to oceanic water masses (Table 4.1 and Figures 4.1 and 4.2, Longdill *et al.*, 2005). In addition, discrete bottle samples were obtained at selected depths using a 'van Dorn' bottle sampler. Transect surveys were spaced throughout the year to obtain a picture of seasonal dynamics and observe the 3-dimensional nature of the hydrodynamics and water column structure. Surveys were completed within 2-3 days, with individual transect lines taking between 3-10 hours, allowing horizontal patterns over the area from a single survey, and vertical slices from individual transects, to be regarded as quasi-

synoptic. On an infrequent basis, weather conditions and instrument problems prevented all transect lines being sampled completely during each survey (Figure 4.2).

Table 4.1 Hydrographic data collection details including, site ID, water depth, sample depth, site location and sampling times within the Bay of Plenty.

Site ID	Water Depth (m)	Sample Depths (m)	NZMGx	NZMGy	Data Collection Times
Moorings: Temperature Sensors					
OPO15	15	1,5,10,15	2884588	6350510	20/03/2004 to 1/08/2004, and 22/10/2004 to 6/12/2004
OPO30	30	1,5,10	2885047	6354233	22/10/2004 to 6/12/2004
OPO40	40	1,5,10,30	2885566	6358296	23/10/2004 to 6/12/2004
OPO65	65	2,8,20	2886665	6367135	26/5/2004 to 1/8/2004 and 4/8/2004 to 22/10/2004
PUK15	15	1,5,15	2828003	6369198	5/12/2003 to 19/3/2004
PUK30	30	1,5,10,30	2830408	6373078	5/12/2003 to 19/3/2004
PUK65	65	2,8,20	2829040	6383170	25/9/2003 to 19/3/2004
Moorings: ADP Deployments					
PUK65	65	6 to 62	2829040	6383170	22/9/2003 to 16/10/2003 and 18/10/2003 to 2/12/2003
OPO25	25	2 – 22	2884804	6352313	19/3/2004 to 8/4/2004
OPO65	65	6 to 62	2886665	6367135	3/6/2004 to 1/8/2004 and 3/8/2004 to 22/10/2004
Field Sampling: CTD Casts					
OPO10	10	0 to 10	2884479	6349415	17/10/03, 3/12/03, 16/3/04, 8/4/04, 25/5/04 and 1/8/04 (± 1 day)
OPO20	20	0 to 20	2884636	6350990	As above
OPO30	30	0 to 30	2885047	6354233	As above
OPO50	50	0 to 50	2886021	6361859	As above
OPO100	100	0 to 100	2887710	6375147	As above
OPO200	200	0 to 200	2888933	6384817	As above
WHK10	10	0 to 10	2862981	6355319	As above
WHK20	20	0 to 20	2863604	6356112	As above
WHK30	30	0 to 30	2865348	6359499	As above
WHK50	50	0 to 50	2867899	6363124	As above
WHK100	100	0 to 100	2875140	6376649	As above
WHK200	200	0 to 200	2877580	6380890	As above
PUK10	10	0 to 10	2827892	6369054	As above
PUK20	20	0 to 20	2828533	6370066	As above
PUK30	30	0 to 30	2830408	6373078	As above
PUK50	50	0 to 50	2832774	6376884	As above
PUK100	100	0 to 100	2838278	6385687	As above
PUK200	200	0 to 200	2840189	6388745	As above
Field Sampling: Water Samples					
OPO10	10	1	2884479	6349415	17/10/2003, 3/12/2003, 16/3/2004, and 25/5/2004 (± 1 day)
OPO20	20	1, 20	2884636	6350990	As above
OPO30	30	1, 20, 30	2885047	6354233	As above
OPO50	50	1, 20, 30, 50	2886021	6361859	As above
OPO100	100	1, 50, 100	2887710	6375147	As above
OPO200	200	1, 20, 30, 50, 200	2888933	6384817	As above
WHK10	10	1	2862981	6355319	As above
WHK20	20	1, 20	2863604	6356112	As above
WHK30	30	1, 20, 30	2865348	6359499	As above
WHK50	50	1, 20, 30, 50	2867899	6363124	As above
WHK100	100	1, 50, 100	2875140	6376649	As above
WHK200	200	1, 20, 30, 50, 200	2877580	6380890	As above
PUK10	10	1	2827892	6369054	As above
PUK20	20	1, 20	2828533	6370066	As above
PUK30	30	1, 20, 30	2830408	6373078	As above
PUK50	50	1, 20, 30, 50	2832774	6376884	As above
PUK100	100	1, 50, 100	2838278	6385687	As above
PUK200	200	1, 20, 30, 50, 200	2840189	6388745	As above

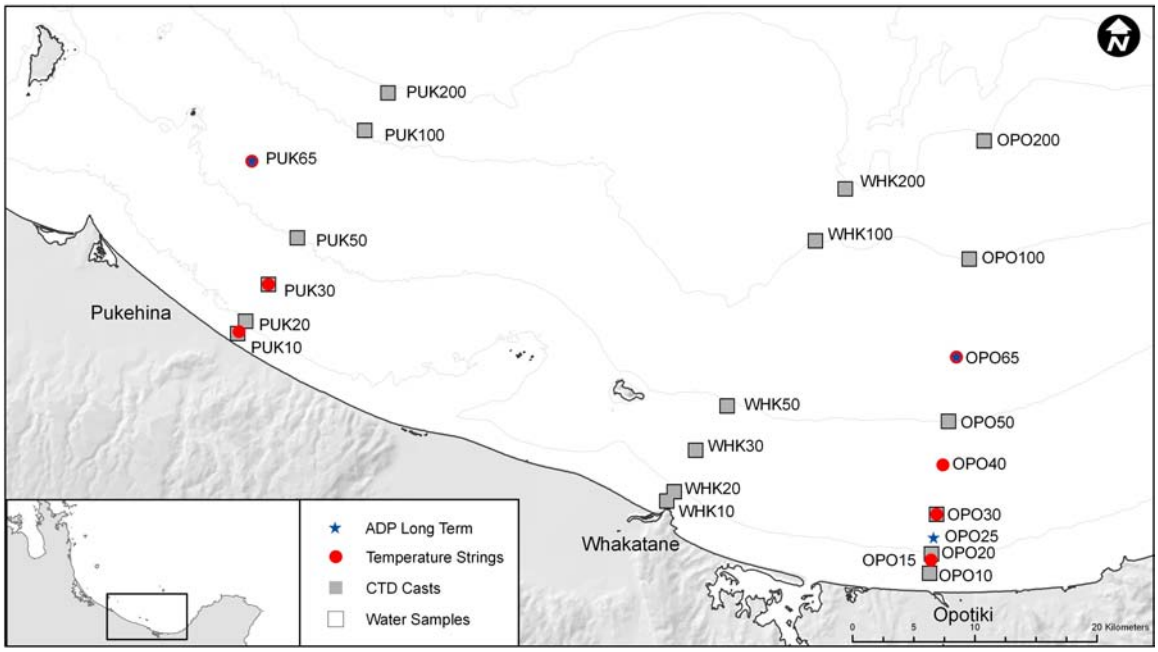

Figure 4.1 Location of hydrographic sampling stations within the Bay of Plenty. The Pukehina 65 m site used for ADP deployment was not located directly on the Pukehina transect due to potential interference with commercial trawlers. (see also Table 4.1 and Figure 4.2).

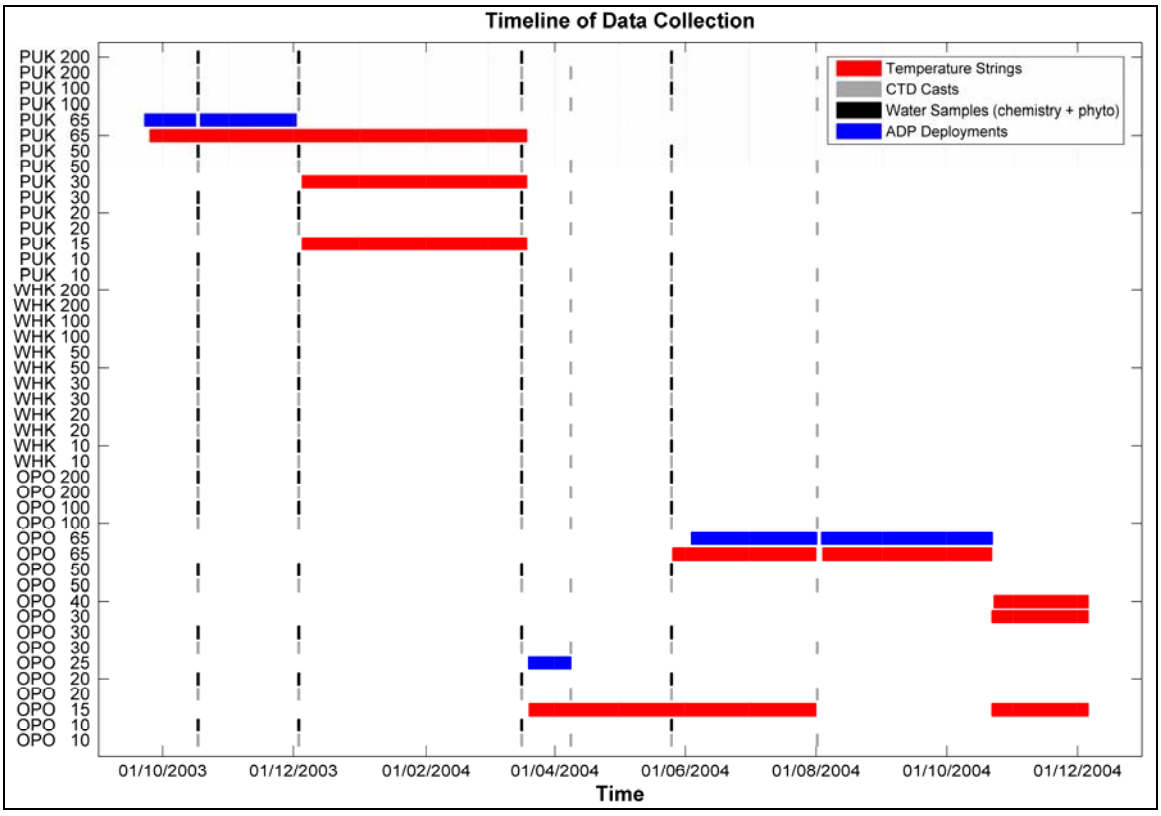

Figure 4.2 Timeline of collection of hydrographic data within the Bay of Plenty (see also Table 4.1 and Figure 4.1).

4.4.1 CTD PROFILES

Profiles of salinity, temperature, oxygen, fluorescence and suspended sediments were obtained with a SEABIRD® SBE 19+ Seacat Profiler (SBE43 oxygen sensor, TURNER SCUFA fluorometer and Optical Backscatter Sensor). Calibration of the

CTD temperature, conductivity (salinity), and dissolved oxygen probes was undertaken at the EBOP laboratory according to the manufacturer's guidelines during December 2002 (temperature and conductivity) and November 2003 (dissolved oxygen). Calibration of the fluorometer using 29 filtered and analysed water samples returned an R^2 value of 0.86 corrected for turbidity. CTD data were interpolated along the shore normal transects using SURFER® 7.0 and a krigging algorithm over a 300 m (horizontal) by 3 m (vertical) grid.

These data shall be used to indentify the structure of the shelf water column during different seasons and also to provide essential data to calibrate 3-dimensional numerical models of both hydrodynamics and ecosystem dynamics of the shelf environment.

4.4.2 WATER COLUMN CHEMISTRY

Water samples were collected concomitantly with the CTD casts using a 3.0 L van Dorn bottle at targeted depth intervals at each station along the transects (Table 4.2). As a quality control measure the temperatures and salinities of the collected water samples were measured and recorded immediately upon collection with an YSI30 hand held salinity/conductivity/temperature meter.

Table 4.2 Sampling strategy for water samples to be analysed for nutrients, chemistry and phytoplankton. xx indicates sampling position.

		Station Depth (m)					
		10	**20**	**30**	**50**	**100**	**200**
Sample Depth (m)	**0-5**	xx	xx	xx	xx	xx	xx
	20		xx	xx	xx		xx
	30			xx	xx		xx
	50				xx	xx	xx
	100					xx	
	200						xx

Laboratory analyses were conducted by Environment Bay of Plenty (EBOP), with phytoplankton counts processed by the National Institute of Water and Atmospheric Research (NIWA). Analyses followed standard methods for all constituents (Table 4.3). Data were plotted along shore normal transects after gridding using SURFER® 7.0 and a triangulation with linear interpolation scheme over a grid of 3000 m (horizontal) and 15 m (vertical) resolution.

These data shall be used to characterise nutrient delivery to the shelf ecosystem and also to calibrate a 3-dimensional ecological model of the Bay of Plenty shelf.

Table 4.3 Methods used for the analysis of water column chemistry and phytoplankton.

Parameter	Method	Detection Limit†
Suspended Solids	APHA method 2540D (APHA, 1998)	0.1 $g.m^{-3}$
Total nitrogen	Persulphate digestion, auto cadmium reduction, flow injection analyser APHA 4500-NO3,4500-P (APHA, 2005)	1.0 $mg.m^{-3}$
Ammonium nitrogen	Phenolhypochlorite colorimetry (NWASCO, 1982)	1.0 $mg.m^{-3}$
Oxidised nitrogen	Flow injection analyser, APHA 4500 NO3-1 (APHA, 1998)	1.0 $mg.m^{-3}$
Total Phosphorus	Acid persulphate digestion, molybdate colorimetry. Flow injection analyser. APHA 4500-PH (APHA, 1998)	4.0 $mg.m^{-3}$
Dissolved Reactive Phosphorus	Antimony – phosphate – molybdate (NWASCO, 1982)	4.0 $mg.m^{-3}$
Chlorophyll-a total filterable	Total phytoplankton filterable on 0.7µm and above, GFC filtration, acetone pigment extraction, spectrofluorometric measurement	0.1 $mg.m^{-3}$
Nano-chl-a	As for total Chlorophyll-a but only for plankton 0.7-20µm	0.1 $mg.m^{-3}$
Micro-chl-a	As for total Chlorophyll-a but only for plankton 20-200 µm	0.1 $mg.m^{-3}$

†Detection limit with 95% confidence, some results do not reach this level

4.4.3 TEMPERATURE STRINGS

Thermistor arrays (StowAway® TidbiT® sensors) were deployed during separate time periods along the Pukehina and Opotiki transects throughout the water column (Figure 4.1 and Table 4.1). A lead weight attached to the surface line immediately below the deepest thermistor kept the line taught and the sensors at a constant depth relative to the surface. Several early strings were lost due to either deliberate cutting or fouling in a propeller of the line below the surface float. Subsequently, a mooring system with backup retrieval method was developed using a crown anchor along with surface and subsurface floats. The thermistors recorded ambient water temperature every hour on the hour during the deployments. Several thermistor strings were lost due to either accidental or intentional interference. Figure 4.1 and Table 4.1 show only those deployments where data (and instruments) were recovered. The resulting data (no concurrent data at Pukehina and Opotiki) limits conclusive abilities with respect to the along-shelf extent of any observed patterns and dynamics.

The temperature string data are to be used, along with CTD, current meter, water sample and meteorological data to in an attempt to quantify shelf dynamics. Additionally these data shall be used to calibrate a 3-dimensional baroclinic numerical model of shelf hydrodynamics.

4.4.4 ADP MOORINGS

Current speed and direction data were recorded by a single SONTEK® 500KHz Acoustic Doppler Profiler (ADP) and averaged over a 10 minute interval each hour (Table 4.4). The single ADP was rotated around the sites, meaning that at any one time currents could only be measured at one site. This limits the interpretation of these data c.f. multiple concurrent instrument deployments and the spatial extent of large flow features remains somewhat unknown. The ADP mooring was deployed

through spring 2003 at the Pukehina 65 m site, for a short period in autumn 2004 at the Opotiki 25 m site and during winter/spring 2004 at the Opotiki 65 m site (Figure 4.2). The ADP was deployed on a bottom mounted frame linked by a 70 m ground line to a 200 kg crown anchor (Beamsley *et al.*, 2005). The crown anchor had a direct link to a large steel radar reflecting surface buoy with a flashing light to act as a warning to vessels. The ADP frame was also linked directly to a smaller surface buoy, with temperature sensors attached to this line. This line allowed the ADP to be serviced and downloaded without the need to lift the large 200 kg crown anchor to the surface. The 500 kHz APP returned acceptable signal to noise ratios over a distance of 61 m from the ADP head.

Table 4.4 SONTEK ADP setup for the ADP deployments.

Instrument type	SONTEK
Frequency	500 kHz
Serial number	C522
Blanking distance	1.0 m
Cell size	2.0 m
No. of cells	30
Averaging interval	600 s (10 mins)
Profiling interval	3600 s (1 hour)
Co-ordinate system	East, North, Up
Horizontal velocity uncertainty	± 0.09 $cm.s^{-1}$

The current meter data is to be used to characterise the shelf water column response to wind forcings and subsequent relationships with water column temperature profiles. Additionally, these data are used to calibrate a numerical model of shelf physical dynamics. Many of the analyses using these data involved rotating the current vectors to orient with the local bathymetry and coastline. To facilitate this, a standard right hand co-ordinate system was adopted with positive y values being directed offshore, and positive x values along-shelf to the right of an observer looking seawards. Local bathymetric orientation was taken as the mean orientation of 10 km segments from the 10, 20, 30, 40, 50, 60, 70, 80, 90, 100, and 200 m depth contours.

4.4.5 REMOTELY SENSED SST

Remotely sensed SST data, derived from the Advanced Very High Resolution Radiometer (AVHRR), were obtained at 1 km spatial resolution from the National Institute of Water and Atmospheric Research Ltd (NIWA) in netCDF format. Instantaneous SST retrievals in the dataset have a standard deviation error of ~0.6^{o}C and a bias error less than ±0.1^{o}C (Richardson *et al.*, 2005). Climatological (inter-annual) monthly means, produced from monthly composites (1993 – 2004) of these data were processed using a Fourier decomposition method (Uddstrom and Oien, 1999). Cloud detection algorithms, SST retrieval equations, compositing method and a broad scale validation are detailed in Uddstrom and Oien (1999) and Richardson *et al.* (2005).

A validation, specific to the study region, of the 3-day averaged SST data using both thermistor and CTD data over a period of several months at 18 separate locations indicate that the remotely sensed SST provides an accurate representation of the measured data at the 95% confidence level (Figure 4.3).

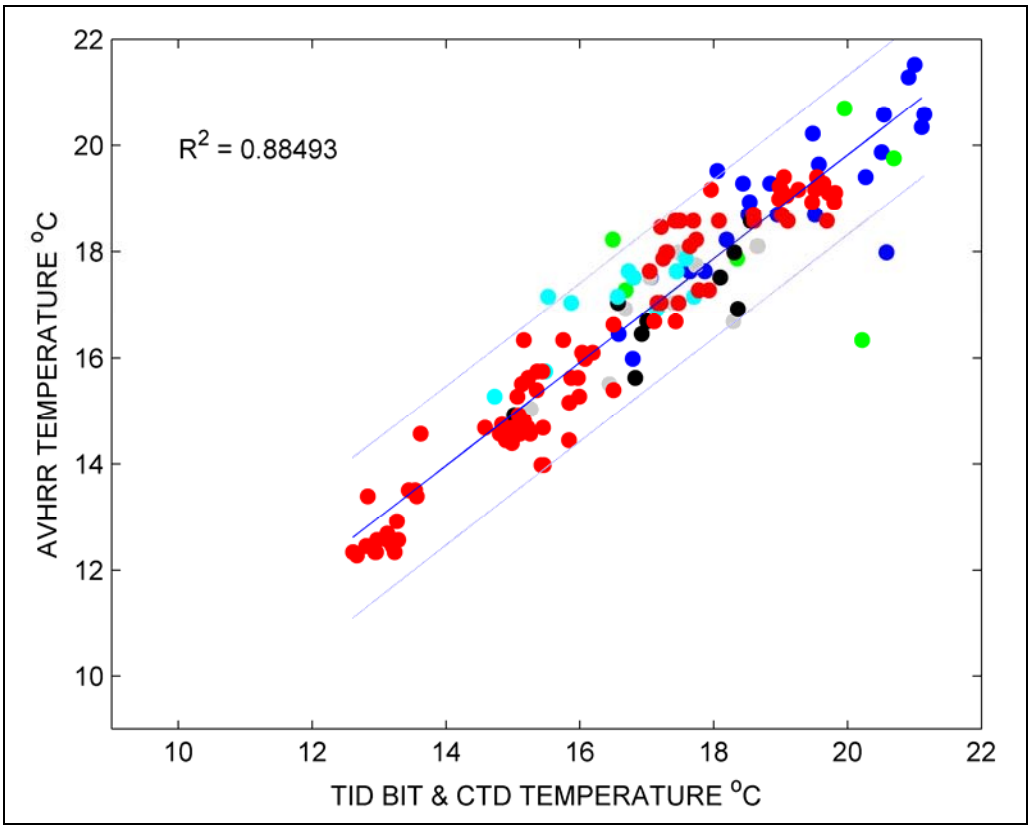

Figure 4.3 Regression of remotely sensed (3 day average) and measured (TIDBIT® temperature probes and SEABIRD® CTD casts) SST within the Bay of Plenty for periods between 2003 and 2005, n=149. Data was obtained from 18 separate sites along three independent cross-shelf transects. Tidbit temperature sensors located at 1 or 2 m water depth, CTD temperatures taken as the average of the upper 5 m. Red dots signify CTD comparisons at 12 different locations, while other colours indicate thermistor data with one colour per site. Solid line indicates linear fit and dashed lines are 95% confidence limits for new observations.

4.4.6 REMOTELY SENSED CHL-A

Remotely sensed climatological monthly mean CHL-a data (1997-2004), derived from the Sea-viewing Wide Field-of-view Sensor (SeaWiFS) were obtained at both 4 km and 1 km resolutions from NIWA. Case 2 CHL-a products were generated using the NIWA Inherent Optical Properties (IOP) algorithm to iteratively solve a set of non-linear equations in order to both correct for non-phytoplanktonic sediment concentrations and to retrieve IOP from corrected water leaving radiances (Richardson *et al.*, 2005). The NIWA IOP algorithm (Pinkerton *et al.*, 2006) was calibrated and validated for the Bay of Plenty region based on an extensive field survey of bio-optical parameters within the study area (Pinkerton *et al.*, 2005). Details regarding the calibration of the algorithm for the study region are recorded in Pinkerton *et al.* (2005).

A local calibration (Pinkerton *et al.*, 2005; Richardson *et al.*, 2005) of the Case 2 IOP algorithm (*e.g.* Lavender *et al.*, 2004; Pinkerton *et al.*, 2006; Smyth *et al.*, 2006) for the specific properties within the Bay of Plenty consisted of a 6 day survey of 24 sites during June 2004 to measure in-situ Chl-a, suspended sediment and dissolved detritus. Though the calibrated IOP Case 2 results were deemed to '*not differ from the in-situ values at the 95% confidence level*' (Richardson *et al.*, 2005), a more spatially and temporally rich comparison with an independent dataset (calibrated CTD casts) does not support these claims (Figure 4.4), and even indicates errors greater than the ±35% error inherent in the sensor (Lavender *et al.*, 2004). Potential explanations for the poor comparison include:

a) the patchy distribution of phytoplankton in coastal waters, with CTD samples representing a point location and remotely sensed data covering a much larger 1x1 km cell;

b) the very restricted temporal range of the data used to calibrate the algorithm (6 consecutive days, Richardson *et al.*, 2005) and the resulting lack in variation of measured values of Chl-a ($0 – 2$ mg.m^3) which were available to calibrate the IOP algorithm; and

c) poor performance of the IOP algorithm. The IOP algorithm, when applied to remotely sensed data, has been found to fail in 90% of pixels due to the underestimation of some wavelengths by the SeaWiFS sensor (Lavender *et al.*, 2004).

From these data (Figure 4.4) it can be concluded that the remotely sensed Chl-a data processed with the methodology of Pinkerton *et al.* (2005) and Richardson *et al.* (2005) are inaccurate in their ability to infer nearshore (< 100 m depth) Chl-a values in the Bay of Plenty. The authors themselves acknowledge some weaknesses in these data products when they conclude that '*a quantitative estimate of the errors from the IOP algorithm is not possible*' (Richardson *et al.*, 2005). These data products should be used with caution as they are at best only likely to provide qualitative information on the distribution of surface chlorophyll where Case 2 conditions are important.

An assessment of the within pixel variation of the remotely sensed Chl-a data is not possible from the current data set as CTD casts and water samples were spaced farther apart than the 1 km^2 resolution of the SeaWifFs data.

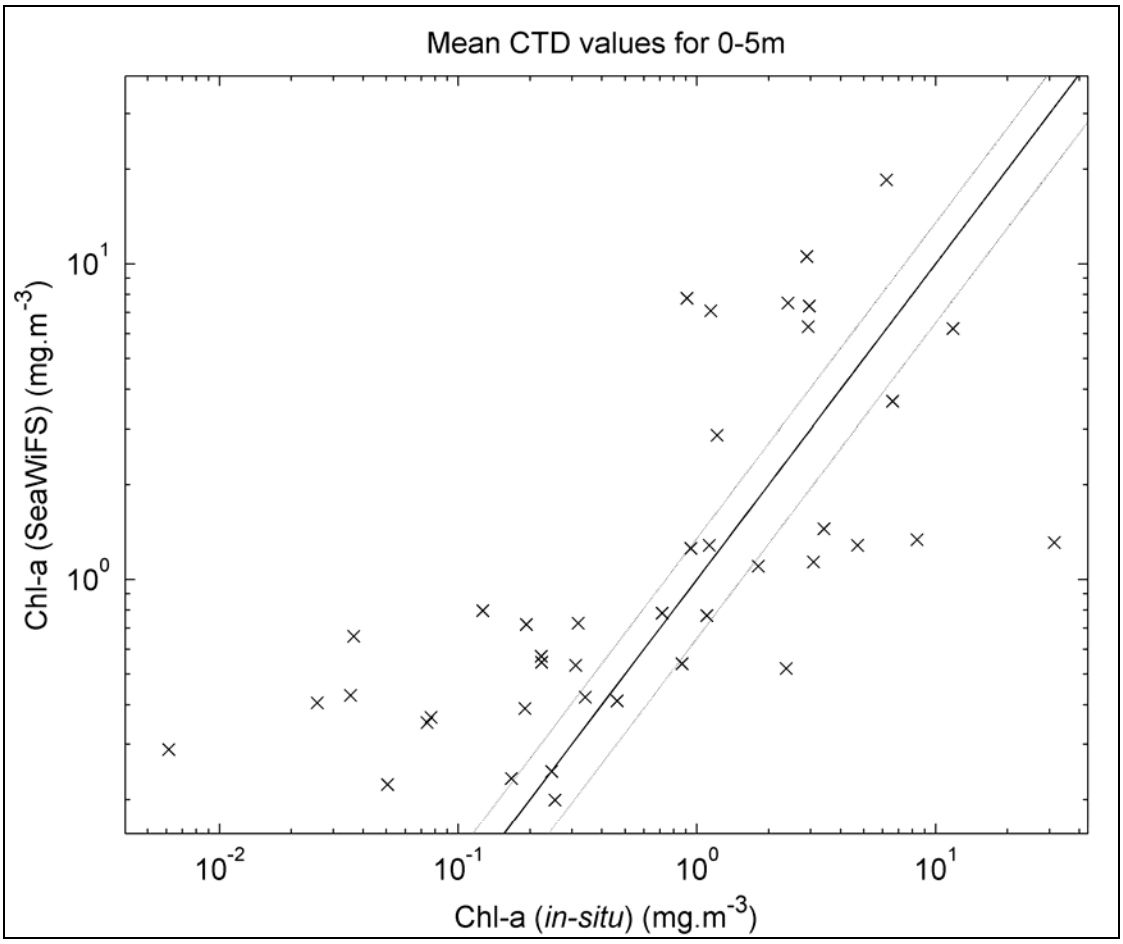

Figure 4.4 Comparison of remotely sensed Case 2 Chl-a values (from Bay of Plenty specific IOP algorithm) and values from a calibrated CTD (calibrated with filtered water samples and turbidity measurements). CTD values represent the average value of the upper 5 m of the water column, and are within the 1 km cell of the remotely sensed data. The 1:1 line is shown solid and the light grey lines indicate the ±35% error range of the SeaWiFS sensor.

4.4.7 METEOROLOGICAL DATA

Meteorological data (wind vectors, air temperature, barometric pressure, humidity, solar irradiance) were obtained as hourly time series from Tauranga and Whakatane airports. Additionally, wind vectors were obtained from QuikSCAT nodes within the Bay of Plenty. The SeaWinds instrument, on the sun-synchronous orbiting QuikSCAT satellite, is a specialised radar measuring near-surface wind speed and direction with ~25 km resolution (Lungu, 2006). Generally, this results in twice per day coverage over the Bay of Plenty. Wind retrievals are provided on a 25 x 25 km spatial scale with an accuracy of 2 ms^{-1} and 20^o for the level 2B Science Data Products (SDP) used (Lungu, 2006).

4.5 THERMAL CHARACTERISTICS OF THE BAY OF PLENTY SHELF

4.5.1 SPATIAL AND TEMPORAL PATTERNS

Typically, SSTs throughout the year within the greater Bay of Plenty exhibit a pattern of increasing temperatures with increasing distance from shore (Figure 4.5), a pattern also identified by Ridgeway and Grieg (1986) from a single 'snapshot' in February, 1981 using discrete water samples. The temperature gradient is stronger (Figure 4.5) and more consistent (Figure 4.6) in the winter months (June, July, and August) than during summer period (December – March). During the winter months, when strongest shore-normal temperature gradients exist, the cooler nearshore waters typically extend from Matakana Island in the west to Te Kaha in the East (Figure 2.3 and Figure 4.5). The low standard deviations of the means over these areas during the winter months indicate the relative consistency of this pattern (Figure 4.6).

During the summer months, when the shore normal gradient in temperature is somewhat weaker, the cool nearshore water is typically separated by a 'tongue' of warmer water extending from the offshore water mass to the shore adjacent to Te Kaha in the eastern Bay of Plenty (see January and December, Figure 4.5). Accompanying standard deviations indicate that the cool nearshore regions have the greatest variability in temperature throughout the Bay of Plenty during these months (Figure 4.6).

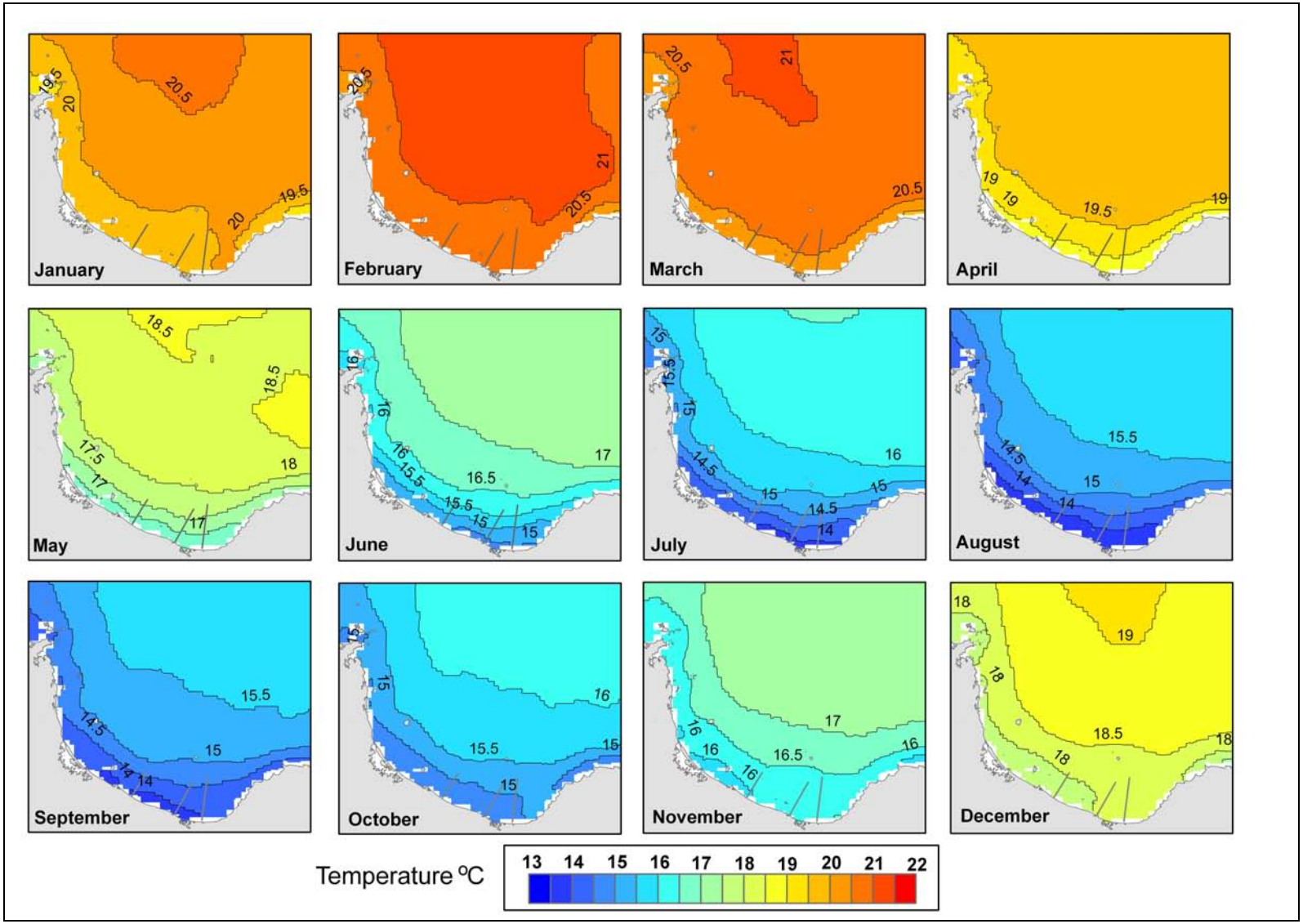

Figure 4.5 Monthly mean SSTs (°C) within the Bay of Plenty inferred by AVHRR radiometer between January 1993 and December 2004. CTD transects shown as grey lines (from west to east, Pukehina, Whakatane, Opotiki).

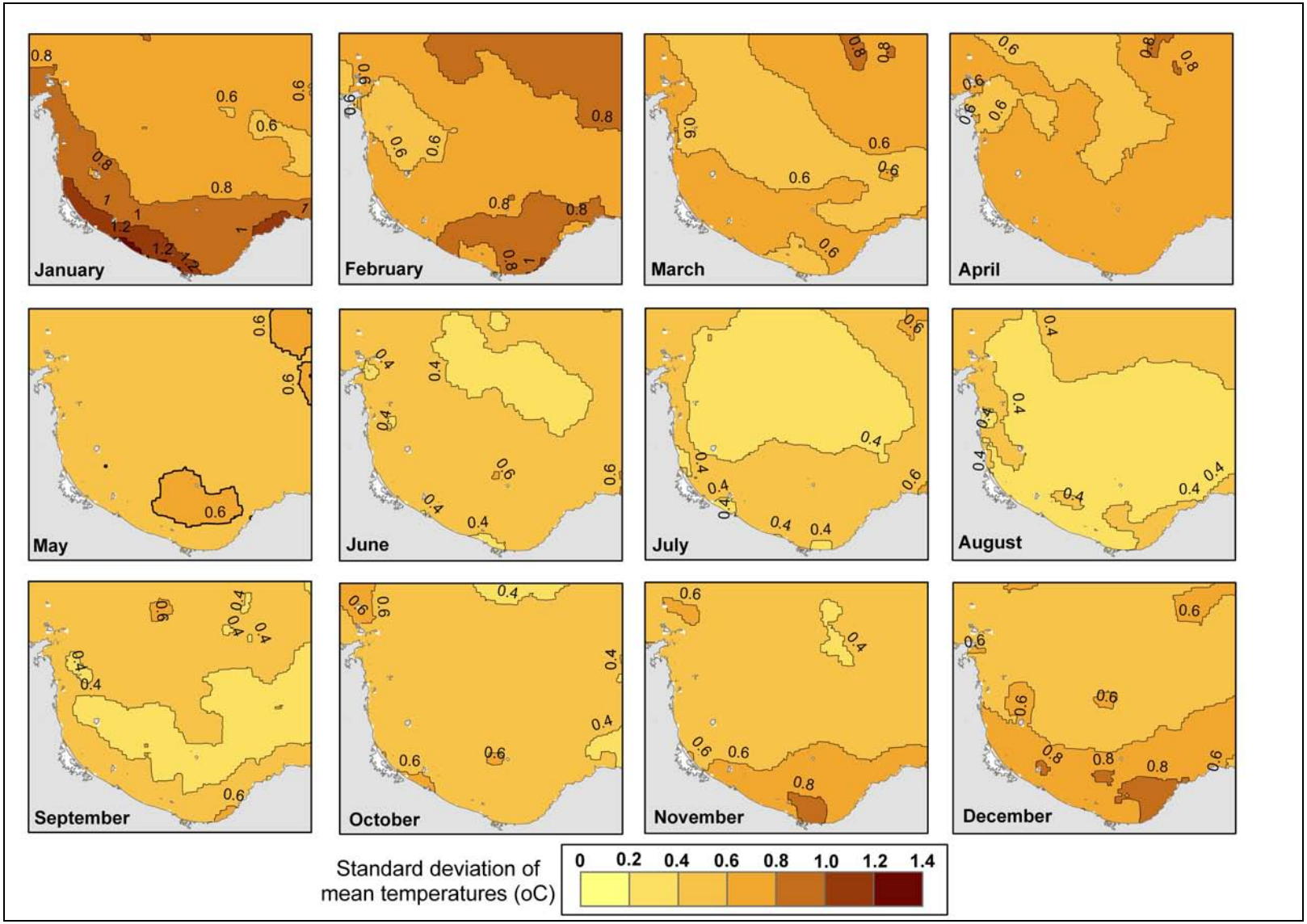

Figure 4.6 Standard deviations of monthly mean SSTs within the Bay of Plenty between January 1993 and December 2004.

Maximum mean SSTs of between 21 and 21.5 ^{o}C occur in offshore waters whilst minimum mean temperatures of between 13.5 and 14 ^{o}C are most prevalent in shallower nearshore waters from Matakana Island to Te Kaha (Figure 4.5). Annual SST maxima generally occur in February and minima in August (Figure 4.5), a pattern consistent with other locations around New Zealand (Heath, 1985; Grieg *et al.*, 1988). The mean annual range in SST within the Bay of Plenty varies from 5.25^{o}C in the offshore regions to 7^{o}C in the nearshore regions of Opotiki (Figure 4.7), again consistent with previous studies within New Zealand waters (Heath, 1985; Grieg *et al.*, 1988; Bell and Goring, 1998).

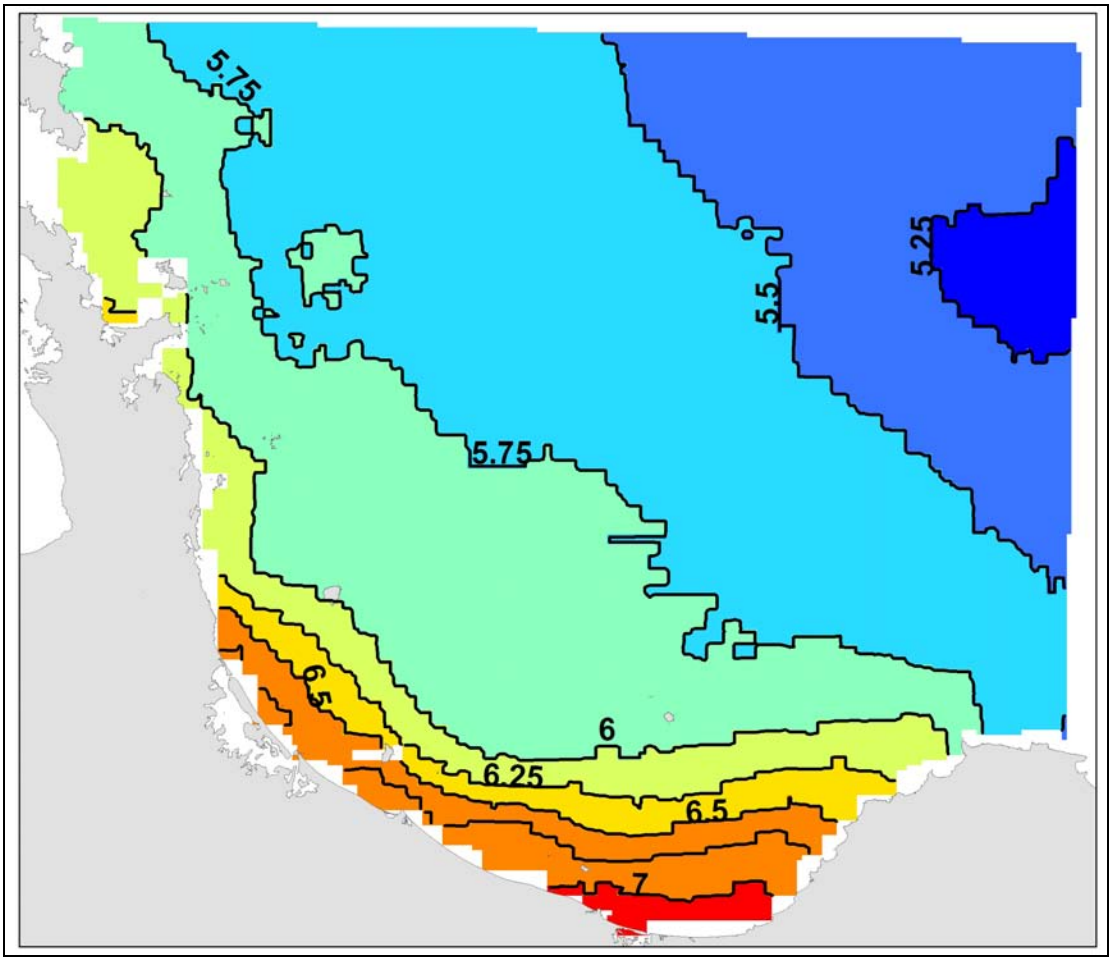

Figure 4.7 Mean annual range in SST within the Bay of Plenty between 1993 and 2004. Range calculated from maxima and minima within each pixel from the inter-annual monthly mean data (Figure 4.5).

4.5.2 THERMOCLINE DEVELOPMENT

CTD surveys during 2003/4 indicate that the temperature of the top ~150 m of the water column across the continental shelf varies seasonally, with the effect decreasing with depth (Figure 4.8). The water column was well mixed during October 2003, with stratification well underway in December 2003 when the thermocline was located at a consistent ~30 m depth. Stratification became more pronounced throughout the summer months with warm (>15^{o}C) water extending to ~100 m depths, a pattern consistent with that offshore from the Hauraki Gulf (Sutton and Roemmich, 2001).

The Opotiki transect exhibits a more defined warm surface layer during March 2004 than do the other transects. This pattern is consistent with the location of a 'warm tongue' of water which persists over this location during the summer months (Figure 4.5). The strong thermal stratification had broken down by May 2004, and in August 2004 an inverse thermal profile was present. It is likely that this inverse stratification is a result of an exceptional flooding event which took place throughout the Bay of Plenty (Whakatane, Rangitaiki, Tarawera and Waioeka Rivers) between 15 and 18 July, 2004, two weeks prior to the CTD survey. Strongly reduced salinities within the surface layer at this time (see accompanying CD-ROM) provide further evidence for this hypothesis and indicate that this inverse thermal structure may not be a regular or consistent phenomenon.

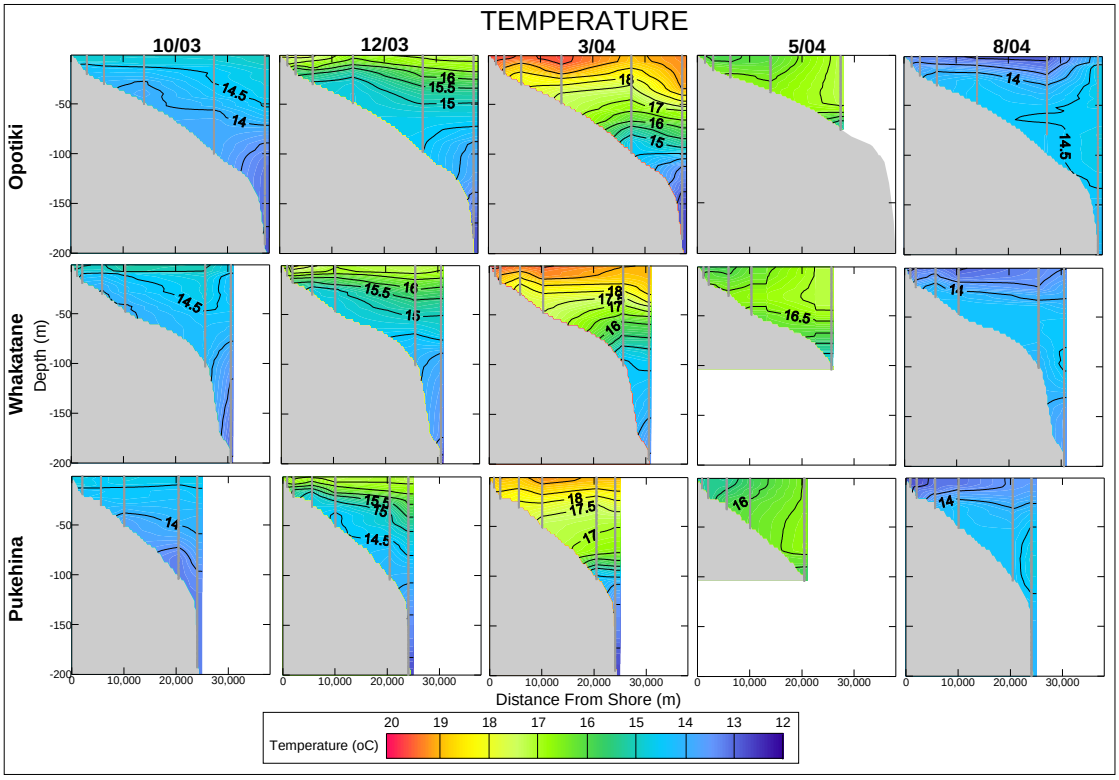

Figure 4.8 Temperature profiles along shore normal transects from CTD casts. CTD data points shown as grey dots, data gridded using a krigging algorithm with a resolution of 3000 m (horizontal) and 3 m (vertical), without extrapolation.

4.5.3 NEARSHORE STRATIFICATION

Detailed analyses of water column stratification from temperature moorings along the Pukehina transect reveal relatively rapid changes in the degree of stratification of the water column, over time periods of approximately one week (Figure 4.9). At all sites (15 m, 30 m, and 65 m depths) strong stratification develops during December 2003, however, just as rapidly the water column is mixed during late December and early January (to a depth of at least 30 m, Figure 4.9). A rapid cooling of the water column takes place during February 2004, which along with a large influx of freshwater, mixes the entire water column to a depth of at least 30 m and at least as far offshore as the 65 m depth contour.

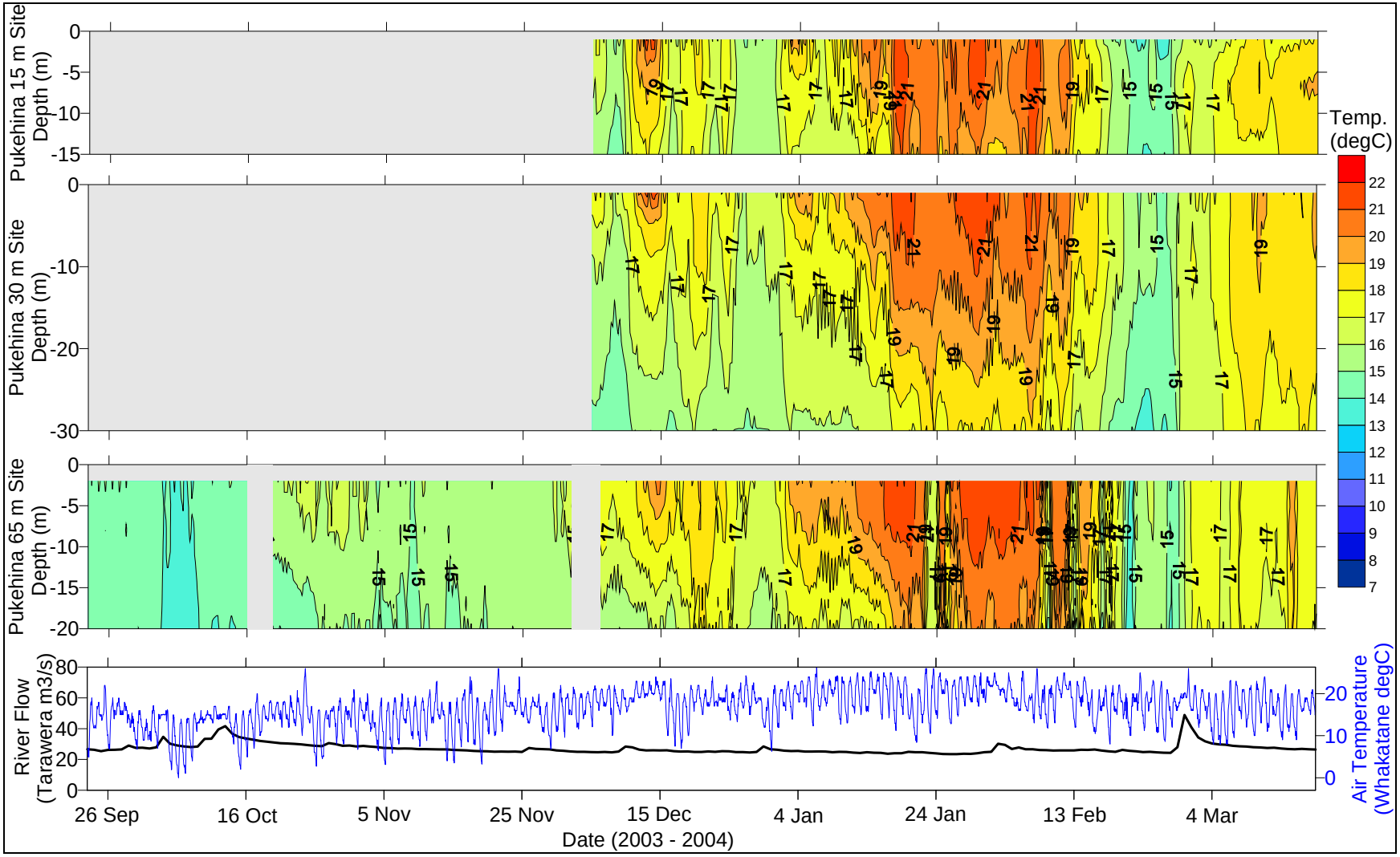

Figure 4.9 Water column temperatures along the Pukehina transect between September 2003 and April 2004 (low pass filtered with a 4 hour running mean filter). Temperatures recorded by TidBit® temperature sensors hourly at 1, 5 and 15 m depths (15m site), 1, 5, 10 and 30 m depths (30 m site), and 2, 8, and 20 m depths (65m site). The instrument at the 65 m site was serviced in October and November. River flows from the nearby Tarawera River (daily gaugings) and air temperature from Whakatane Airport (hourly measurements).

Throughout the winter months, the 65m site along the Opotiki transect is well mixed to a depth of at least 20 m, the only exception being during early August, where the surface waters are cooler than those 20 m below (Figure 4.10). This Bay wide pattern (Figure 4.8) is thought to be a lagged response to an exceptional flooding event affecting the Whakatane, Rangitaiki, Tarawera and Waioeka Rivers between 15 and 18 July 2004, during which the flow gauge for the Waioeka River failed as a result of the extreme flows (Figure 4.10).

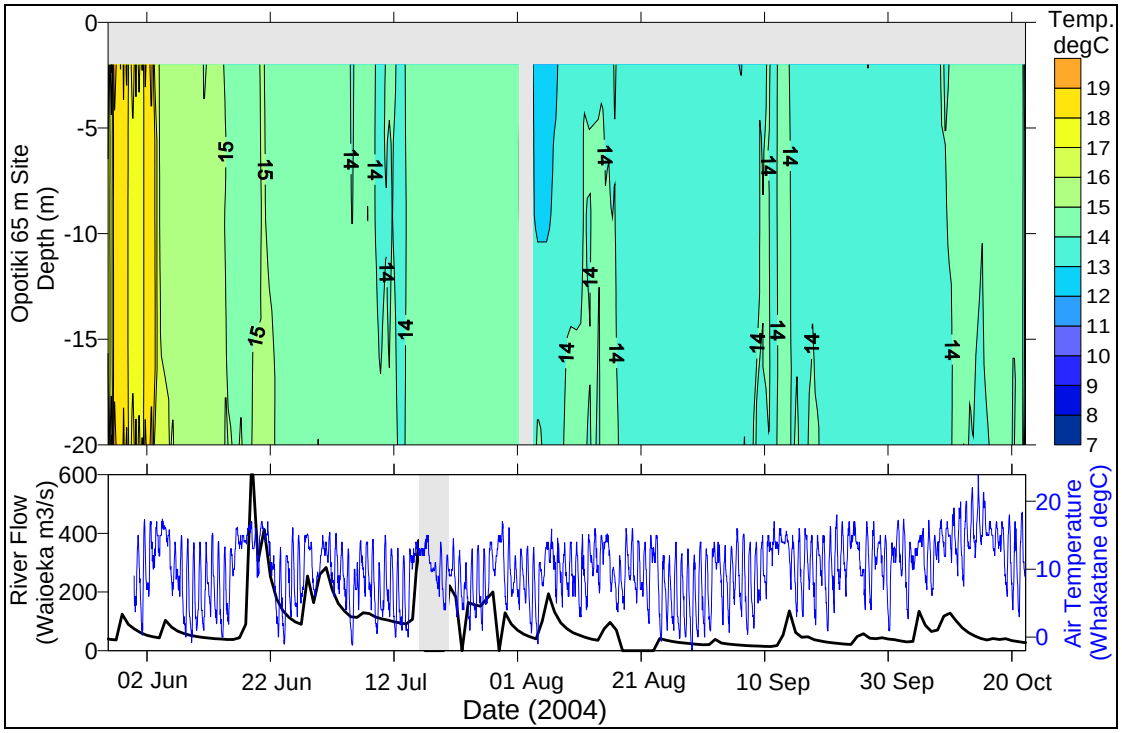

Figure 4.10 Water column temperatures at the Opotiki 65 m site between June 2004 and November 2004 (low pass filtered with a 4 hour running mean filter). Temperatures recorded by TidBit® temperature sensors hourly at 2m, 8m, and 20m depths. Thermistors serviced between 2 and 3 August. Flow gauge malfunctioned between 17 and 20 July 2004 due to extreme flooding event.

Figure 4.11 shows results from the joint deployments at 15, 30, and 40 m along the Opotiki transect. In general there are very few differences between the 15, 30, and 40 m sites during the deployment (Oct-Dec 2004).

During November 2004, the Opotiki transect indicates a stronger level of stratification nearer the shoreline than offshore (Figure 4.11). This stratification is broken up by large flow event from the Waioeka River in mid November 2004 (Figure 4.11). At the 40 m site, the surface temperature is consistently depressed relative to water 5 m below the surface, indicating a persistent inverse stratification not present at either the 15 or 30 m sites.

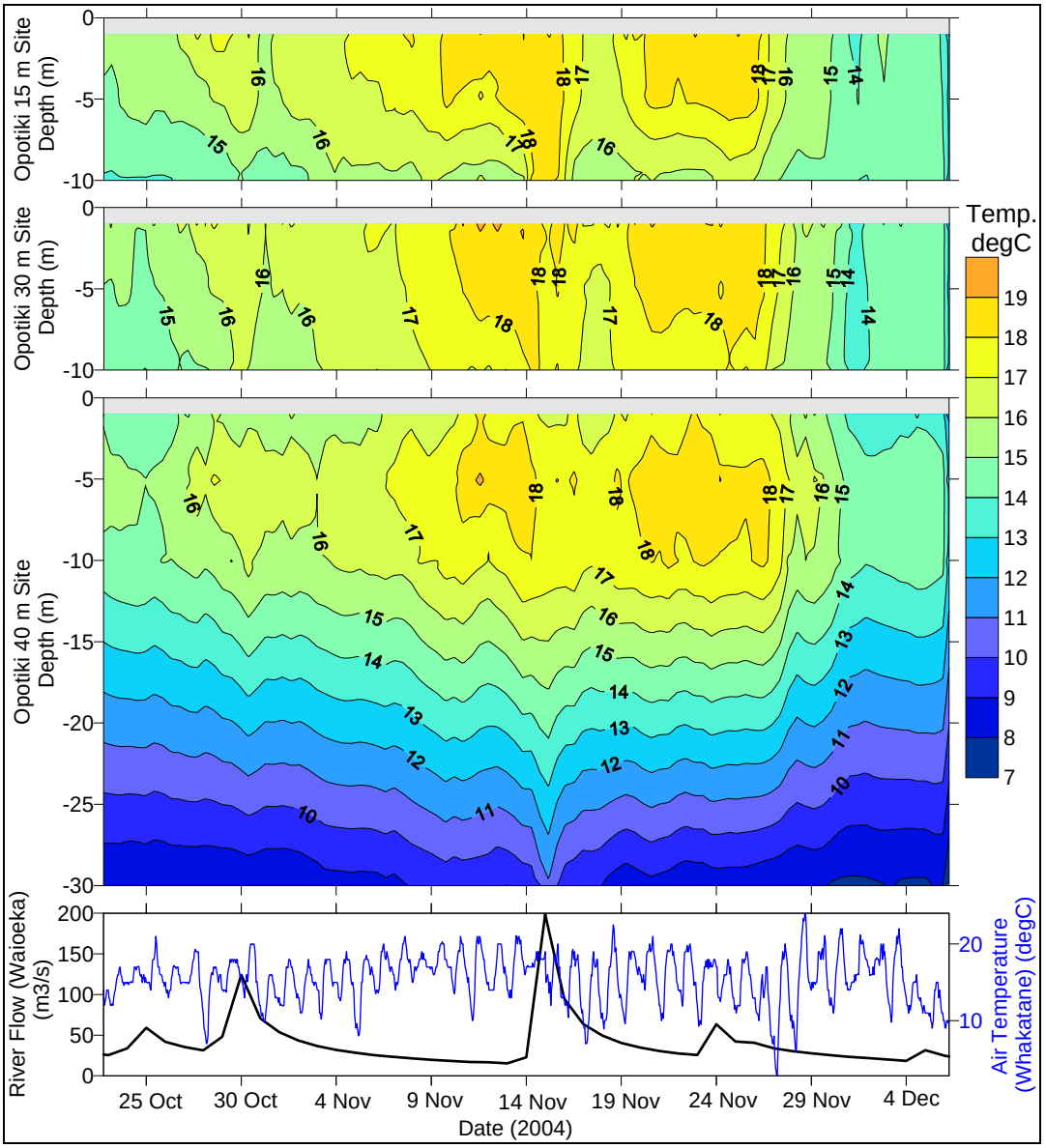

Figure 4.11 Water column temperatures along the Opotiki transect between October 2004 and December 2004 (low pass filtered with a 4 hour running mean filter). Temperatures recorded hourly by TidBit® temperature sensors, located at 1m, 5m, and 10m depths (Opotiki 15m and 30m sites), and at 1m, 5m, 10m and 30m depths (Opotiki 40m site), grey areas indicate no data. River flows from the nearby Waioeka River (daily gauging) and air temperature from Whakatane Airport (hourly measurements).

4.6 OBSERVATIONS OF TIDAL CURRENTS FROM CURRENT METER DATA

4.6.1 DATA PROCESSING

Time series of hourly ADP data from the Pukehina and Opotiki 65 m sites were analysed using T_TIDE software (Pawlowicz *et al.*, 2002) under the MATLAB® environment. This set of programs models the tidal signal as the sum of a finite set of sinusoids at specific frequencies related to astronomical parameters influencing tidal motions. In addition to the amplitude and phase information of each constituent, confidence intervals are provided for each analysed component allowing a robust interpretation of the results (Pawlowicz *et al.*, 2002). Time series of residual currents were determined by removing the tidal signal from the original data.

4.6.2 RESULTS

Tidal current amplitudes are of the order of 2 – 5 cms^{-1} at Pukehina and 2 – 10 cms^{-1} at Opotiki in both along-shelf and cross-shelf directions, near the surface and near the bed (Figures 4.12 and 4.13). At both sites near bed tidal currents vary between similar magnitudes, though display different harmonics to tidal currents nearer the surface (Table 4.5).

Table 4.5 Semi-diurnal (M_2) and diurnal (K_1, O_1) tidal ellipses from the long term ADP deployments. Velocity amplitudes U (along-shelf) and V (cross-shelf) are in cms^{-1}. Phases γ (U-component) and φ (V-component) are in degrees relative to the equilibrium tide at Greenwich. Currents were rotated by 119° (Pukehina) and 85° (Opotiki) to align components with the local bathymetry. Surface currents (s) are the average of those between 3 and 23 m. Bottom currents (b) are the average of those between 43 and 63 m. Only those constituents significant at the 95% level shown.

Current Meter	M_2				K_1				O_1			
	U	γ	V	φ	U	γ	V	φ	U	γ	V	φ
PUK65(s)	0.92	225	2.53	288	2.20	258	2.60	23	1.66	171	1.02	273
PUK65(b)	0.98	186	2.90	258	1.35	223	0.73	313	2.31	203	1.57	321
OPO65(s)	1.59	279	2.67	282	3.83	100	1.58	214	2.27	46	1.66	171
OPO65(b)	1.57	277	2.83	283	3.36	117	2.65	256	2.03	57	1.73	193

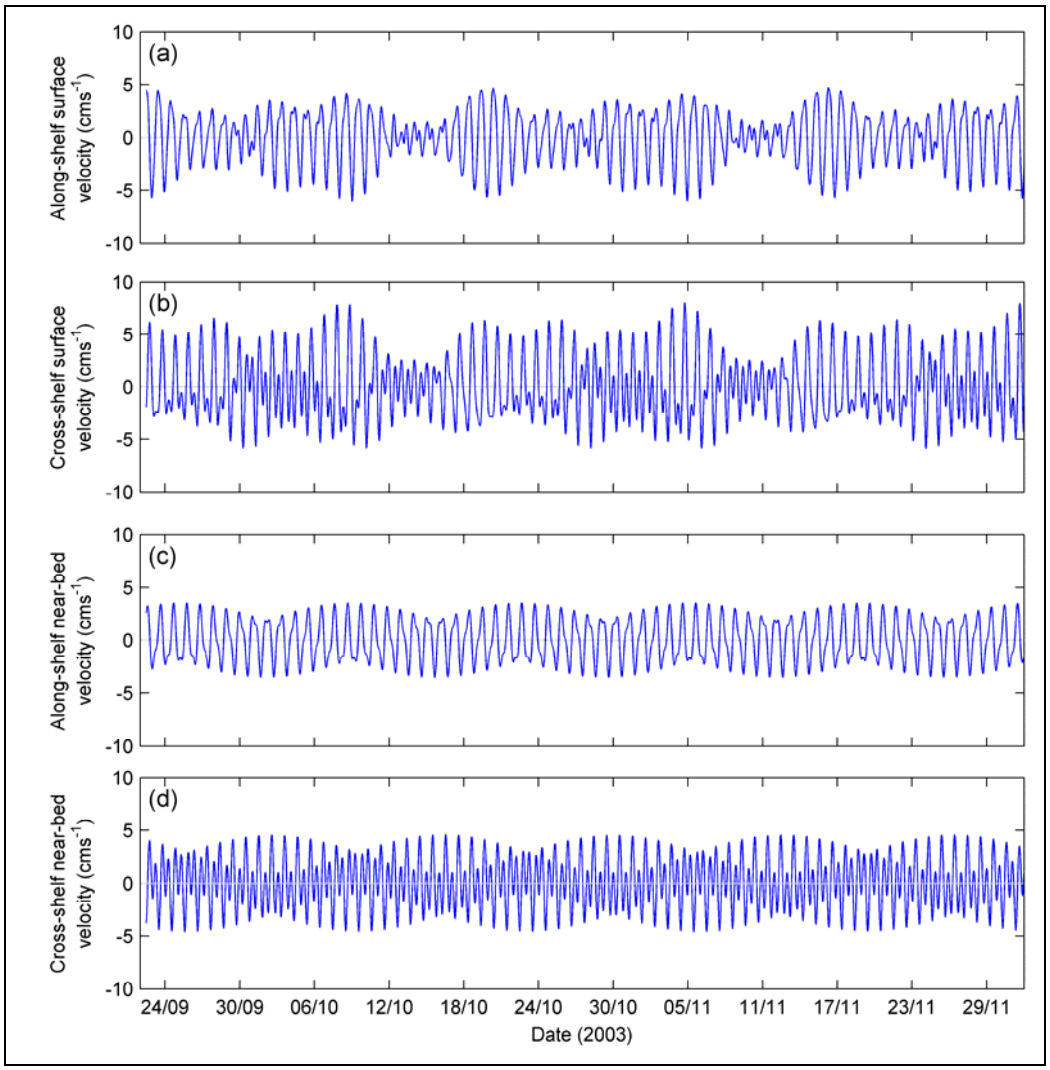

Figure 4.12 Tidally influenced velocities at Pukehina 65 m site from a 70 day record of ADP data. Velocities have been rotated by 119° to align with the local bathymetry. ADP bins have been averaged over the surface (3 – 23 m depth, (a) and (b)) and near bed (43 – 63 m depth, (c) and (d)).

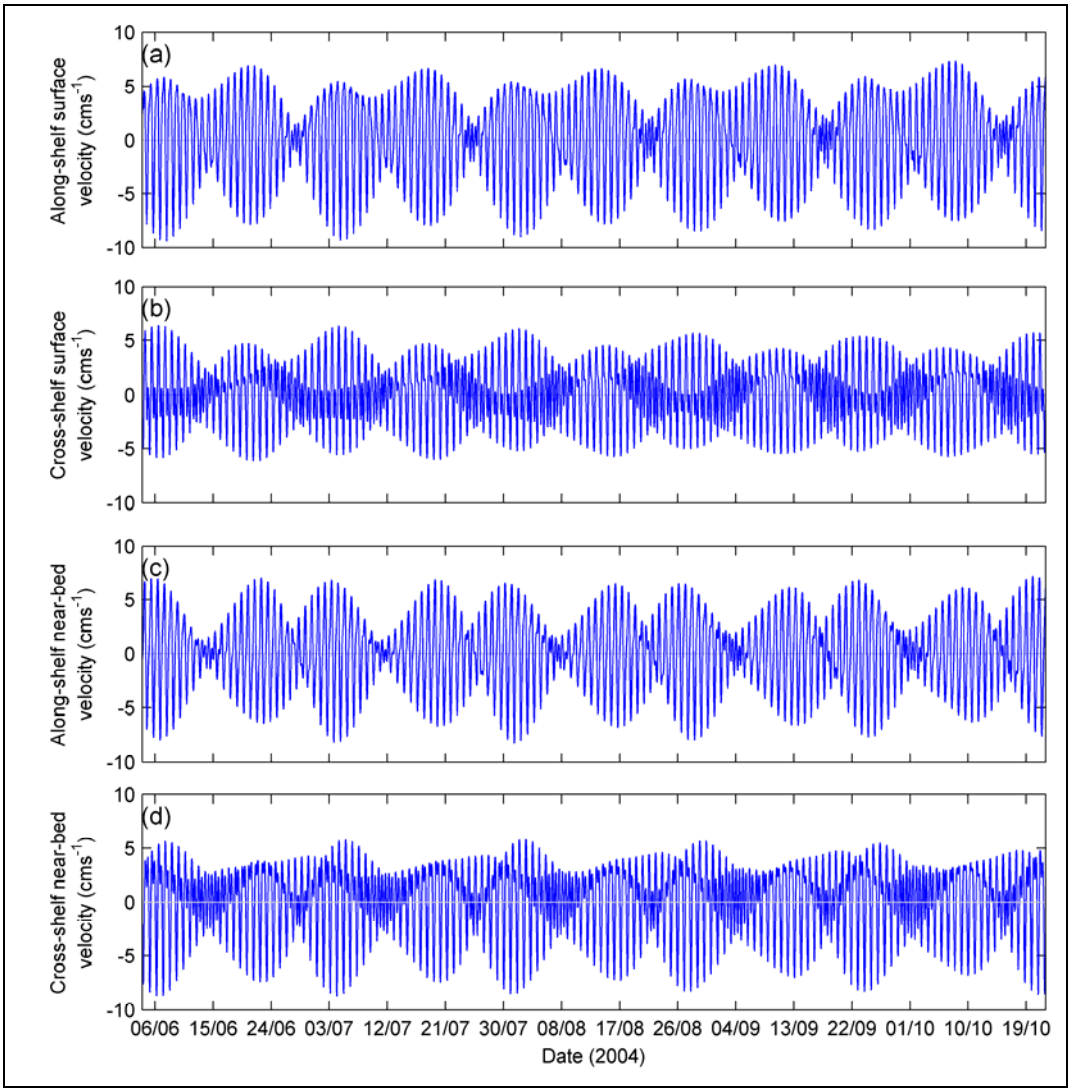

Figure 4.13 Tidally influenced velocities at Opotiki 65 m site from a 140 day record of ADP data. Velocities have been rotated by 85° to align with the local bathymetry. ADP bins have been averaged over the surface (3 – 23 m depth, (a) and (b)) and near bed (43 – 63 m depth, (c) and (d)).

Separation of the record into statistically significant (95% level) individual constituents (Table 4.5 and Figure 4.14), indicate that the tidally influenced currents are dominated by a combination of the M_2, K_1, and O_1 components (principal lunar semi-diurnal, principal lunar-solar diurnal, and the lunar diurnal constituents respectively). M_2 tidal current ellipses were oriented perpendicular to the shoreline and local bathymetry, with very similar surface and near-bed current velocities at both Pukehina and Opotiki sites (Table 4.5 and Figure 4.14). K_1 and O_1 ellipses are oriented more shore parallel at both sites, have similar surface and near-bed current velocities (with the exception of the K1 currents at Pukehina), and notably are of similar magnitudes to the M_2 ellipses. All significant constituents rotate in an anticlockwise direction.

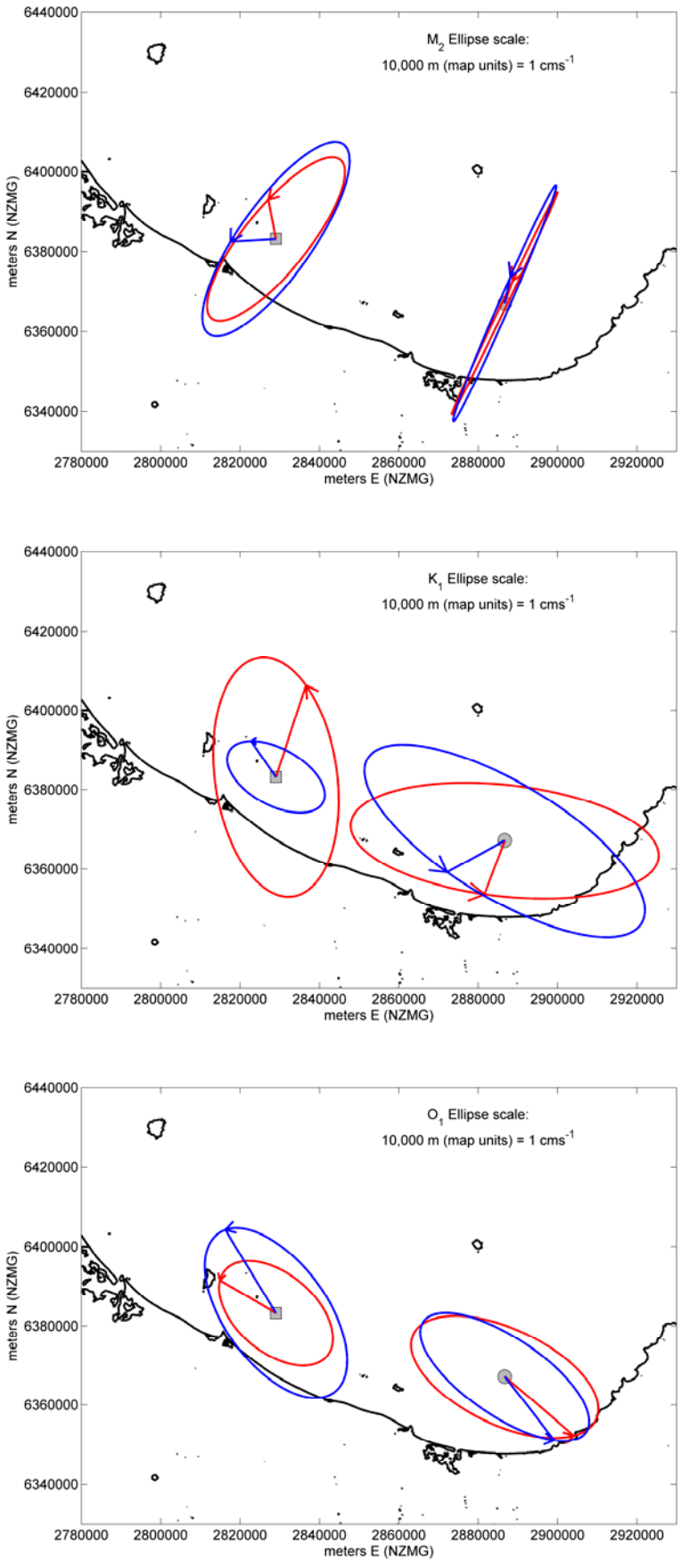

Figure 4.14 M_2, K_1, and O_1 tidal ellipses from the Pukehina 65 m site (grey square) and the Opotiki 65 m site (grey circle). Red ellipses represent the surface flows (3 and 23 m depth) and blue ellipses represent the near-bed flows (43 and 63 m depth). Arrows indicate the direction of flow, and the line represents the phase relative to the equilibrium tide at Greenwich.

4.6.3 DISCUSSION: TIDAL CURRENT OBSERVATIONS

Tidal currents offshore from Pukehina and Opotiki are somewhat weaker than the 'typical' 10 – 20 cms^{-1} observed on the New Zealand shelf (Stanton *et al.*, 2001). The lack of a significant principal solar semi-diurnal constituent (S_2) at both sites is surprising considering the 70 day (Pukehina) and 140 day (Opotiki) records (separation of S_2 from M_2 requires >14.79 day record). However, the S_2 constituent is known to be weak on the east coast of New Zealand due to the presence of a nearby amphidromic node (Heath, 1985; Stanton *et al.*, 2001; Walters *et al.*, 2001). The K_1 and O_1 diurnal constituents impart a relatively large influence at both sites, being of similar magnitudes to the M_2 constituent. Previously, strong K_1 and O_1 driven flows have been observed nearby at East Cape in current meter data and also predicted by modelling efforts (Stanton *et al.*, 2001). The atypical strength of these diurnal constituents in this region has been attributed to the proximity of an amphidromic node to the east of New Zealand, along with complex interactions with bottom topography and islands (Heath, 1985; Stanton *et al.*, 2001).

Frictional effects generally act to decrease amplitudes and advance the phase of tidal ellipses near the seabed (Stanton *et al.*, 2001). An advance in phase of the near-bed tidal currents is observed only at the Pukehina site with M_2 and K_1 currents, other sites/constituents display either similar or retarded phases at depth (Figure 4.14). Baroclinic (internal) tides can act to complicate expected patterns, and have been observed surrounding New Zealand off the west coast of the South Island (Stanton, 1978; Heath, 1984a; Vennel and Moore, 1993), the north-east shelf (Sharples and Greig, 1998), the Chatam Rise (Chiswell and Moore, 1999) and the Kermadec Ridge (Chiswell, 2000). Baroclinic tides can be identified from vertical structure through the water column of tidal ellipse parameters, specifically the inclination and phase (*e.g.* Vennel and Moore, 1993), or from tidal frequency variation in subsurface temperatures (*e.g.* Sharples and Greig, 1998).

Profiles of ellipse parameters (Figure 4.15) indicate decreasing amplitudes near the bed (within ~15 m) for all constituents, at both sites. There is no evidence of internal tides at the Pukehina site (Figure 4.15 (c) and (d)), or at Opotiki (Figure 4.15 (g) and (h)), with the exception of the K_1 constituent at ~10 m water depth. The phase and inclination shift of this constituent may indicate the presence of an internal tide, however, there is no similar evidence from either the M_2 or O_1 constituents. The Opotiki site was strongly stratified during periods of the deployment due to a buoyant freshwater plume and inverse temperature stratification (Figures 4.8, 4.10, and 4.11) which may have influenced this measurement.

Tidal variability in subsurface temperatures can be caused by either the tidal advection of a horizontal temperature gradient, or the vertical excursion of the thermal structure of the water by an internal tide (Sharples and Greig, 1998). Assuming a typical cross-shelf barotropic current of 5 cms^{-1} (Figures 4.12 and 4.13), the resultant tidal excursion could be up to ~1000 m. Maximum horizontal temperature gradients in the

region (from SST imagery, Figure 4.5) are of the order of $0.04^{o}Ckm^{-1}$, thus tidal frequency variability in the temperature with a greater amplitude ($>0.04^{o}C$) cannot be attributed to horizontal advection, and must be the result of an internal tide. No significant (95% level) oscillations at tidal frequencies greater than $0.04^{o}C$ were found in hourly temperature records from 2, 8, and 20m depths at either site, further discounting the likelihood of internal baroclinic tides being present.

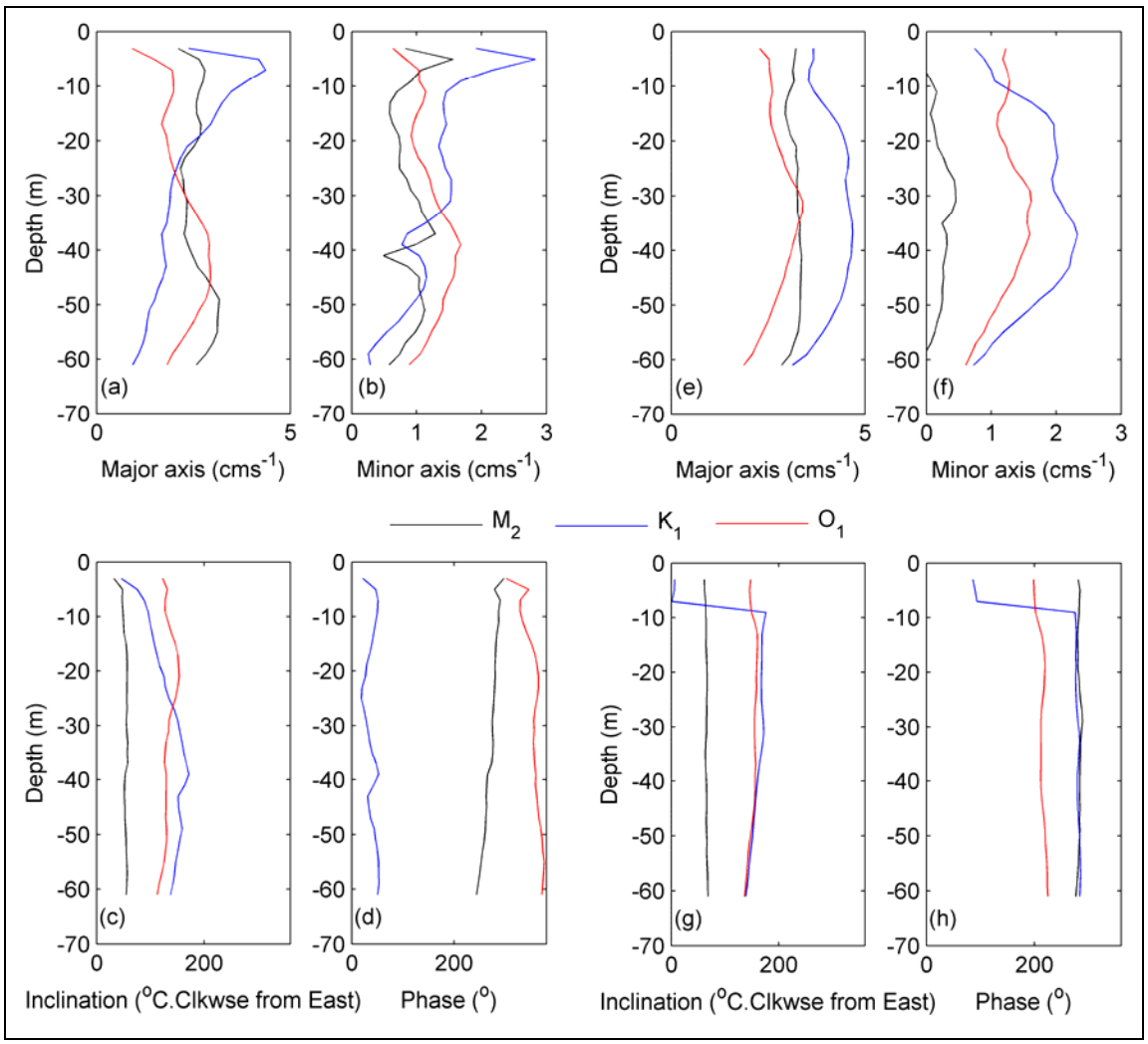

Figure 4.15 Profiles of significant (95% level) tidal ellipse parameters at Pukehina (a–d) and Opotiki (e-h) sites from 70 and 140 day records respectively. Analyses conducted within each 2 m bin of ADP data.

4.7 SHELF CIRCULATION AND TRANSIENT UPWELLING DYNAMICS

4.7.1 OBSERVATIONS OF RESIDUAL CURRENTS

4.7.1.1 CURRENT METER AND WIND RECORD DATA PROCESSING

Time series of non-tidal subinertial residual currents (Figures 4.16 and 4.17) were calculated by removing the tidal signal from the original data and filtering with a low pass filter (36 hour-half power point, *e.g.* Allen and Kundu, 1978; Huyer, 1984 and 1990; Dever, 1997; Tilburg and Garvine, 2003) (throughout this chapter subinertial

will refer to records that have been filtered to suppress both tidal and inertial oscillations, see Dever, 1997). Along-shelf (*u*) and cross-shelf (*v*) components of wind stresses and subinertial currents were calculated oriented to the local bathymetry, with positive *u* directions extending toward 119°T and 85°T, at Pukehina and Opotiki respectively, positive *v* directions are offshore.

Hourly wind speed and direction data were obtained by vector based interpolation of twice daily QuikSCAT data. Wind stress components were calculated using the formulation described by Large and Pond (1981).

Along-shelf flows are typically stronger than cross-shelf flows with variations in flow directions being observed in both component directions at both sites (Figures 4.16 and 4.17). Along-shelf flows are typically consistent in direction throughout the water column, while cross-shelf currents frequently exhibit mid water column reversals in direction (Figures 4.16 and 4.17).

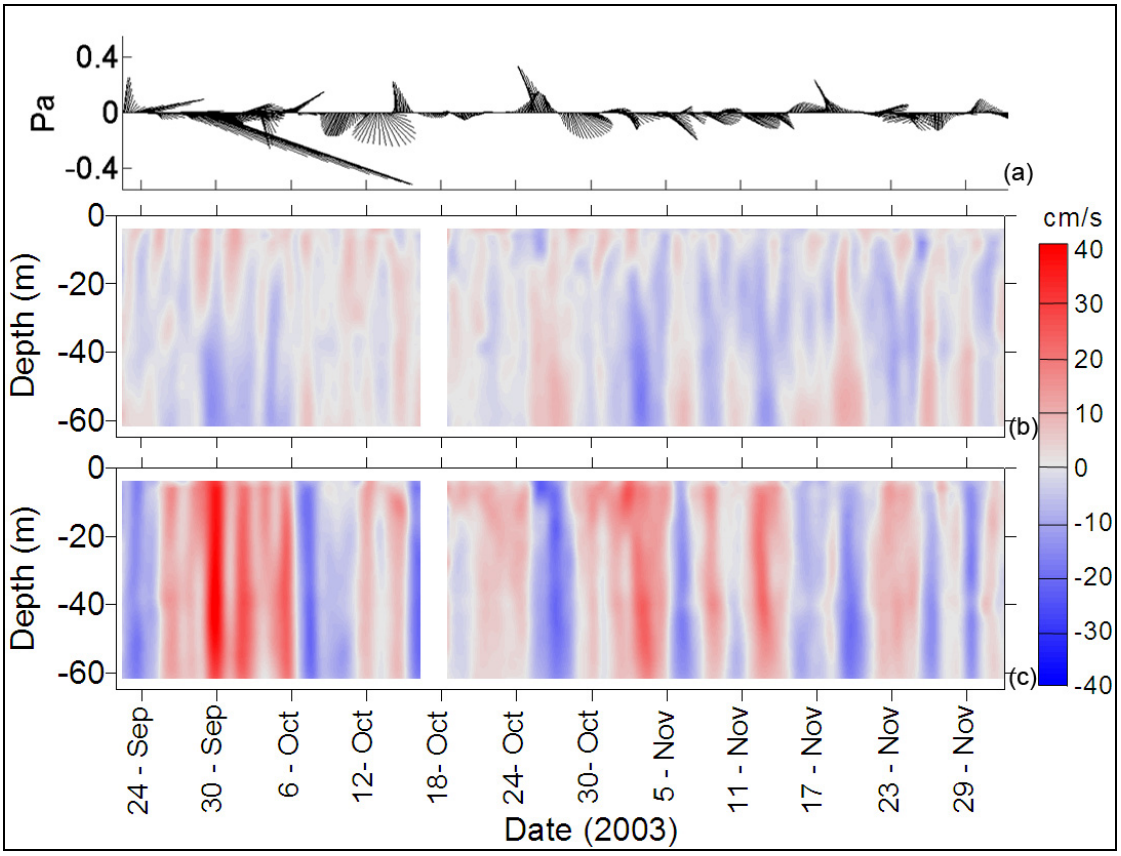

Figure 4.16 Wind stress interpolated from QuikSCAT node at 37.625S, 177.125E (2 data retrievals per day) (a) and contour plot of subinertial cross-shelf (b) and along-shelf (c) velocities (cms^{-1}) at the Pukehina 65 m site. Positive cross-shelf velocities represent offshore flows, while positive along-shelf flows are directed southeastwards along the coast (mean bathymetric orientation of 119°). Instrument was serviced between 16 and 18 October.

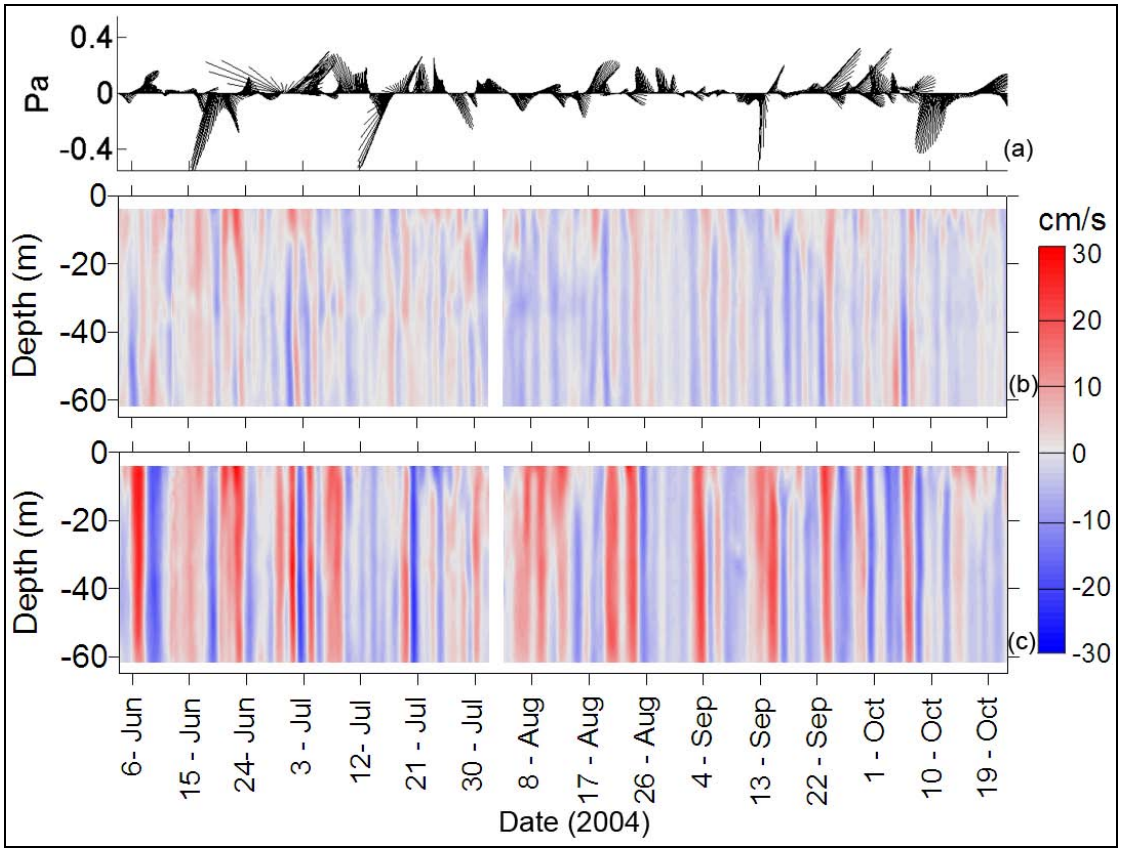

Figure 4.17 Wind stress interpolated from QuikSCAT node at 37.625S, 177.125E (2 data retrievals per day) (a) and contour plot of subinertial cross-shelf (b) and along-shelf (c) velocities (cms^{-1}) at the Opotiki 65 m site. Positive cross-shelf velocities represent offshore flows, while positive along-shelf flows are directed eastwards along the coast (mean bathymetric orientation of 85°). Instrument was serviced between 1 and 3 August.

A basic result of the analysis is that residual flows are typically 20-30 cms^{-1} throughout the water column while tidal flows are typically 2-8 cms^{-1}, indicating that tidal currents play a comparably minor role in influencing overall shelf dynamics, a finding consistent with the outer Hauraki Gulf (Sharples and Grieg, 1998). Also, considering that the available turbulent mixing power of a current is proportional to the mean cube of the current speed, then residual currents will be more than 50 times more effective than tides in providing a mixing force to shelf waters (Sharples and Grieg, 1998).

4.7.2 WIND DRIVEN UPWELLING: PUKEHINA, SPRING 2003

The general NW-SE orientation of the western Bay of Plenty shelf suggests that winds with significant components from the NW and SE should induce upwelling and downwelling circulation patterns over the adjacent shelf. Initial analyses of wind stress, satellite inferred SSTs, and thermistor records offshore from Pukehina during spring indicate this to be a valid hypothesis (Figure 4.18).

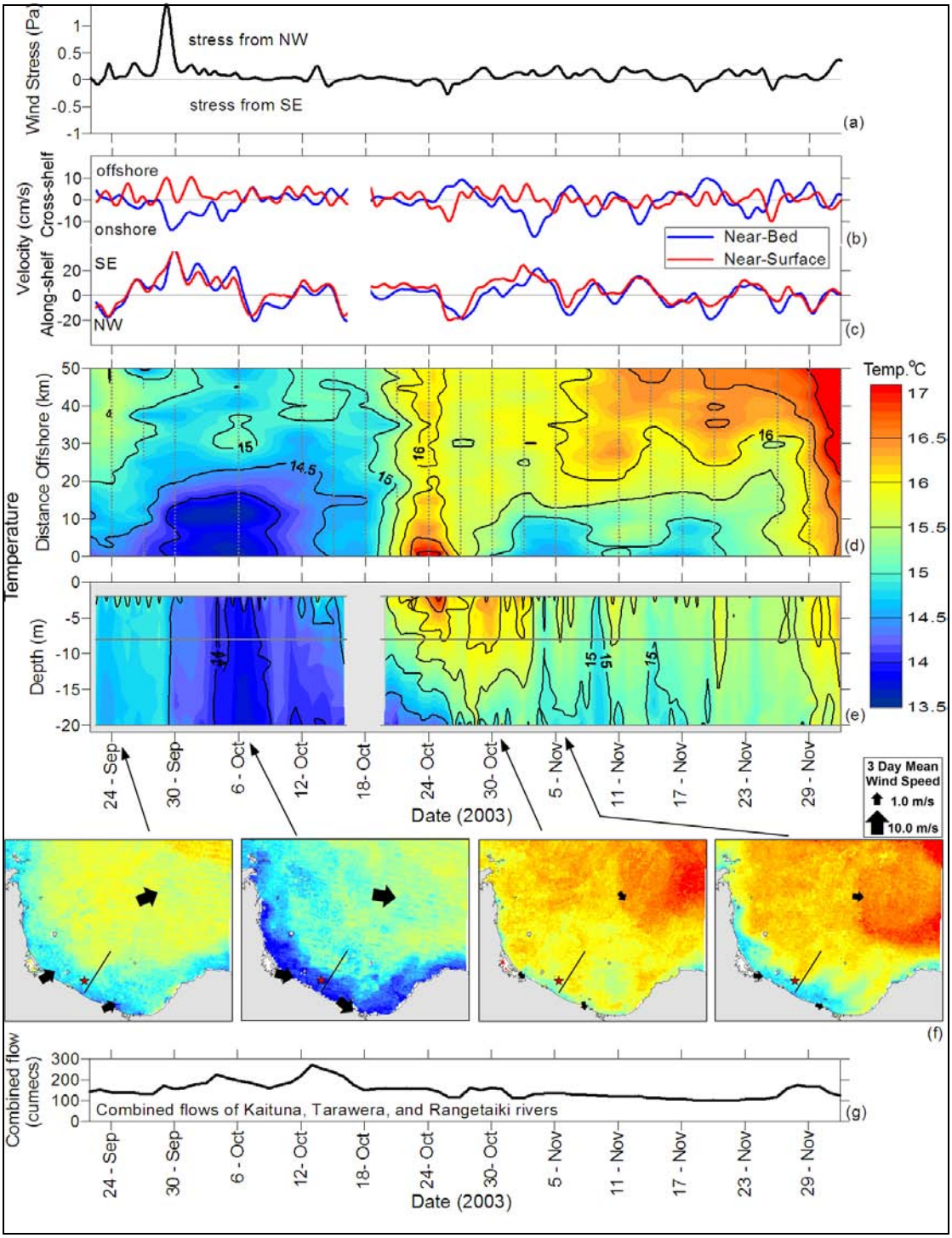

Figure 4.18 Relationships of along-shelf wind stress (Pascals) from QuikSCAT node at 37.625S, 177.125E (a), subinertial cross-shelf (b) and alongshelf (c) near-surface (3-11m, red line) and near-bed residual velocities (43-63m, blue line), sea surface temperatures (^{o}C) from AVHRR (d and f), low pass filtered (butterworth 8 hr) upper-water column temperature-depth profiles at the Pukehina 65 m site (e), and combined river flows of nearby rivers (g). Components based on an mean contour orientation of 119^{o}. In (d), SST data, from a shore normal transect shown in F, were contoured on a 2.5km by 1.5 day grid in offshore distance-time space, positions of raw data indicated by grey dots. In (e) hourly low passed thermistor data were contoured on a 2.5m by 0.5 day grid in depth-time space, thermistors located at 2, 8 and 20 m depths, and were serviced with the ADP between 17 and 19 Oct (b, c and e). In (f) 3-day SST image composites are shown with arrows connecting the images to the middle of the acquisition period, also shown are the corresponding 3-day mean wind vectors from Tauranga and Whakatane airports and QuikSCAT node (a) within the Bay of Plenty. All of (d), (e), and (f) use the same colour scale.

Upwellings:

The largest extended period of wind stress (peak >1.0 Pa) from the NW occurred during late September while a weaker (peak ~ 0.3 Pa) though more extensive period of wind stress from the NW was observed from late October through to mid November 2003 (Figure 4.18a), resulting in strong and weak surface expressions of cool water respectively (Figure 4.18d). Following the peak wind stress during the September event a decoupling between near-surface and near-bed cross-shelf currents occurred (Figure 4.18b). Surface currents moved offshore and near-bed flows moved onshore (Figure 4.18b). Co-incident with this decoupling was the along-shelf displacement of the entire water column in the same direction as the wind stress (Figure 4.18c). Subsequently, a rapid outcropping of cold water to a distance of ~25 km offshore occurred throughout the Bay of Plenty (Figure 4.18d,e,f). The cool surface water persisted for ~12 days following the relaxation of wind stress, before being warmed considerably. This warming (20 – 24 October), recorded in both thermistor and AVHRR data, is not preceded by wind stresses from the SE (downwelling favourable) and is most prominent in nearshore regions (Figure 4.18a,d,e), in conflict with an offshore source indicative of downwelling dynamics. These data do not indicate a shoreward movement of warmer offshore waters, similar to that observed by Sharples (1997) off the northeast of New Zealand. River flows in the area were also unexceptional surrounding this warming period (Figure 4.18g), discounting these as a potential source of warm water.

In the absence of currents (both vertical and horizontal), the required energy gain (Q) to heat the upper 8 m of the water column by an average of 2^{o}C over 6 days (as observed, Figure 4.18e) can be calculated from

$$Q = \frac{(\rho hc\Delta\theta)}{\Delta T} \qquad \textbf{Equation 4.1}$$

with ρ the seawater density (1025 kgm^{-3}), h the thickness of the layer undergoing the temperature change, c the specific heat capacity of seawater (3900 Jkg^{-1}^{o}C^{-1}), $\Delta\theta$ the change in temperature, and ΔT the time over which the temperature change occurred (in seconds). This suggests a net mean heating rate over the 6 days of ~120 Wm^{-2}. The net surface heat flux (neglecting advective components) at the Pukehina site can be estimated from bulk formulae (Pickard and Emery, 1990) using hourly meteorological measurements from the nearby Tauranga Airport. The smoothed net surface heat flux is consistently in the range of +100 Wm^{-2} surrounding this time, indicating it is a probable cause of the observed heating (Figure 4.19), providing advective elements are low (Figure 4.18b,c, 20-26-Oct).

The observed negative surface heat flux at the end of September is at least an order of magnitude smaller than that required to explain the observed cooling in the SST and thermistor records at the same time (depth of cooling extends beyond 20m, Figure 4.18d,e), indicating that advective elements must form a crucial component of the heat balance during this event.

An extended period of 'weaker' (~0.3 Pa) upwelling favourable wind stress occurred between late October and mid November 2003. This stress resulted in periodic decoupling of near-surface and near-bed cross-shelf flows, occurring simultaneously with along-shelf flows to the southeast (Figure 4.18b,c). This weaker event resulted in a more gradual and less severe upwelling event compared to that during late September, with the cool water extending offshore to a distance of ~15 km (Figure 4.18d,e). Heat loss through the surface layers can be neglected as a cause of the observed cooling, as the surface net heat flux (neglecting advective components) was positive throughout these events (Figure 4.19) indicating a net gain of energy by non-advective components. Furthermore, the cooling can be observed to progress upward from depth through the water column (Figure 4.18e), providing evidence supporting a source of deep cool water. This upwelling event was also less dominant in its along-shelf extent than the stronger event of late September, with SST data indicating an absence of cool upwelled water in the region between Opotiki and Te Kaha in the eastern Bay of Plenty (Figure 4.18f).

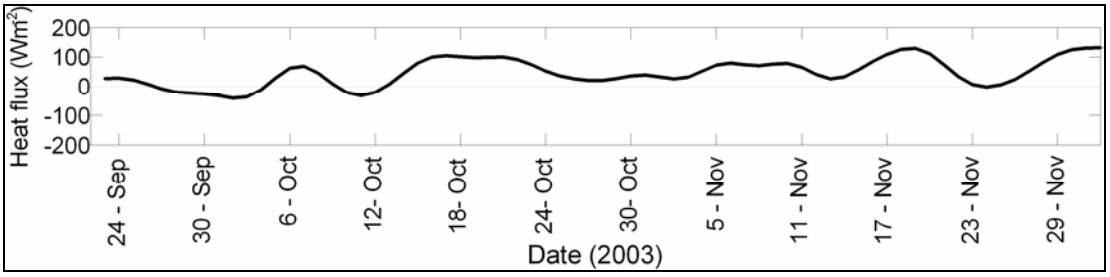

Figure 4.19 Smoothed daily mean sea surface net heat flux (Q_{NET}) in the absence of advection by currents, at Pukehina 65 m site. Based on incoming solar radiation, outgoing long-wave radiation, latent heat of evaporation, and conduction (see Pickard and Emery, 1990).

Downwellings:

On three occasions during the sampling period (26-Oct, 18-Nov, and 26-Nov) the wind stress was directed toward the NW (from the SE) in a direction which may promote the shoreward movement of sub-tropical offshore waters. Sharples (1997) observed that onshore Ekman transport, driven by SE winds during spring, led to the approach of an offshore temperature front towards the shelf edge in the outer Hauraki Gulf. These data provide limited evidence to support this proposition within the Bay of Plenty. Though the wind impulses during the three SE wind events are relatively weak (peak stresses of ~0.2 pa), each is followed by a separation of the cross-shelf near-surface and near-bed flows such that the near-bed currents move offshore and near-surface flows are either directed shoreward (indicative of downwelling) or remain neutral (Figure 4.18a,b). On all three occasions along-shelf currents were directed to the NW (consistent with the wind stress) throughout the water column. While Sharples (1997) observed an increase in temperatures (~2^{o}C over 2 days) due to the shoreward movement of a temperature front, a distinct and similarly rapid increase in surface or sub-surface temperature is not apparent from these data. The Bay of Plenty differs from the outer Hauraki Gulf through the presence of a more diffuse offshore temperature gradient and the absence of a sharp thermal front (> 2^{o}C,

Sharples, 1997) separating the cooler shelf water and warmer subtropical offshore water (*e.g.* Figure 4.18f, image of 30-Oct).

4.7.2.1 NUTRIENT RESPONSE TO UPWELLING EPISODES

Results from the CTD survey of mid October (10 days following strong upwelling) indicate weak upwelling signals in temperature profiles and remarkably high subsurface maxima in Chl-a along all three transects surveyed (>15 $mg.m^{-3}$ at ~ 20 m depth, Figure 4.20). Several studies (including one from the outer Hauraki Gulf) have found that phytoplankton biomass increases only after the relaxation of upwelling circulation (Huntsman and Barber, 1977; Brink *et al.*, 1981; Chang *et al.*, 1992; Chang *et al.*, 2003). It seems a relaxation period is required for bloom initiation, to allow underwater light levels and depleted phytoplankton cells (transported offshore) to increase (Barber and Smith, 1981; Mann and Lazier, 1996; Chang *et al.*, 2003). It is probable that the remarkably high observed subsurface Chl-a concentrations (15 μgL^{-1}) represent the bloom following the relaxation of upwelling conditions, though this observation is limited by the lack of more temporally dense datasets.

Nutrient isopleths at Whakatane and Opotiki displayed characteristic upwelling patterns, with the isopleths shallowing nearer to the shore from beyond the 100 m depth contour (Figure 4.20). Notably, this pattern is more prominent at the Whakatane and Opotiki transects than at Pukehina. If indeed these isopleth patterns are in response to the observed upwelling event of 10 days earlier, it appears that the upwelling persists for a longer period at Whakatane and Opotiki than at Pukehina. Relative to Pukehina, both Whakatane and Opotiki transects are down-flow of the southeastward along-shelf geostrophic current generated during upwelling episodes. As such, the observed patterns may represent the along-shelf displacement of upwelled nutrients.

Concentrations of nutrients in the upwelled water are in the range of 100 – 120 μgL^{-1} NO_X-N, and 18-20 μgL^{-1} DRP (oxidised nitrogen and dissolved reactive phosphorus). These nutrient concentrations underly the Chl-a maxima layer, where significant nutrient reduction is evident.

The December CTD survey immediately followed a short pulse of upwelling favourable winds (Figure 4.18a). Unfortunately, the responses of cross-shelf velocities to this event are unknown due to the retrieval of the ADP on 2 December. AVHRR SST imagery indicates a weak upwelling response which was restricted in spatial extent to the area surrounding the Pukehina transect, with a lack of cool water present at the surface along the Whakatane and Opotiki transects (Figure 4.21). Temperature results from the CTD are suggestive of upwelling with isotherms being compressed near the shoreline. Cool (<15^{o}C) water occurs nearer the surface and closer to shore at Pukehina than at either Whakatane or Opotiki. This observation is consistent with both nutrient (DRP) concentrations (Figure 4.21) and with the bay wide pattern of SSTs, both of which indicate a stronger upwelling signal at Pukehina. Chl-a levels were reduced relative to the October survey with peaks of ~15 and ~8 $mg.m^{-3}$ at Whakatane and Opotiki respectively, occurring at depths of ~20 m.

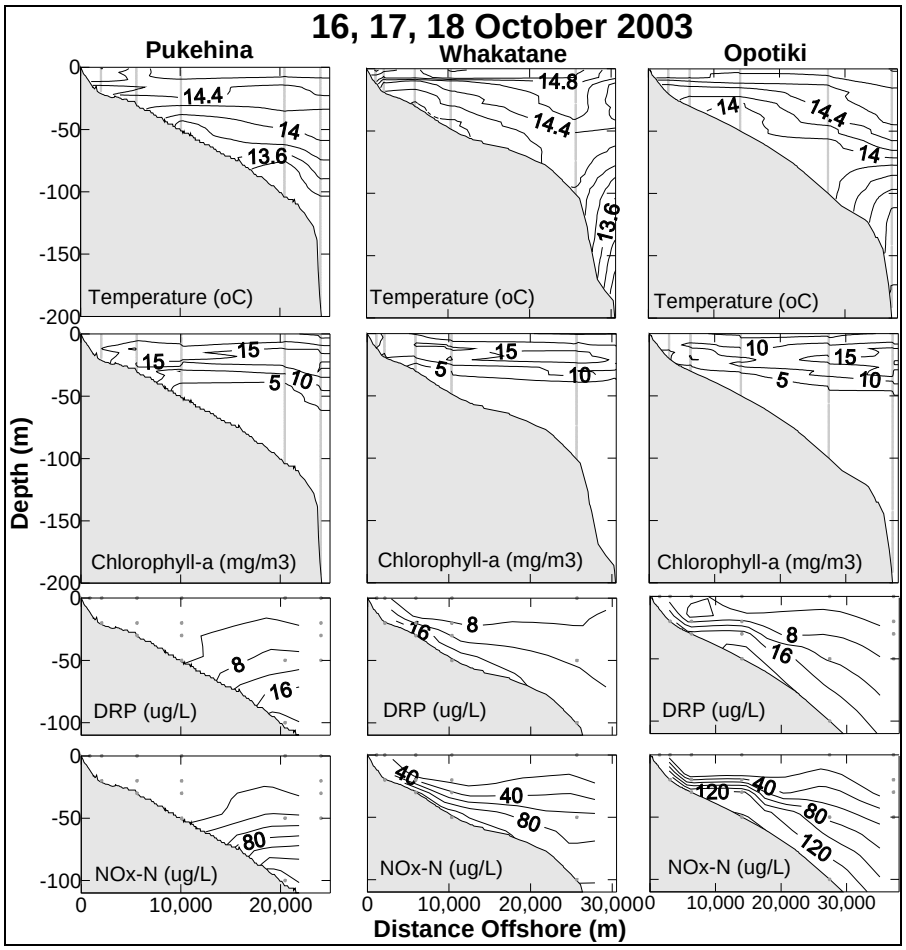

Figure 4.20 Water column temperature and chlorophyll-a from CTD casts, oxidised nitrogen (NOx-N), and dissolved reactive phosphorus (DRP) concentrations from discrete water samples obtained between 16 and 18 October 2003. Data measurement points indicated by grey dots.

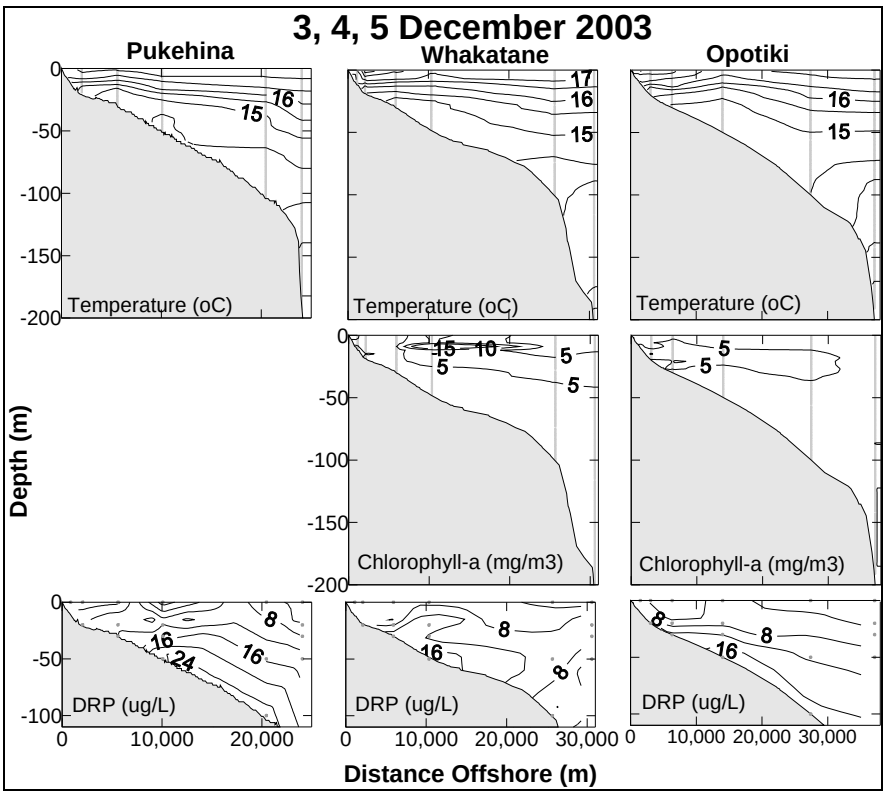

Figure 4.21 Water column temperature and chlorophyll-a from CTD casts and dissolved reactive phosphorus (DRP) concentrations from discrete water samples obtained between 3 and 5 December 2003. NOx-N concentrations were not measured during this survey and the fluorometer failed during the CTD casts at Pukehina. Data measurement points indicated by grey dots.

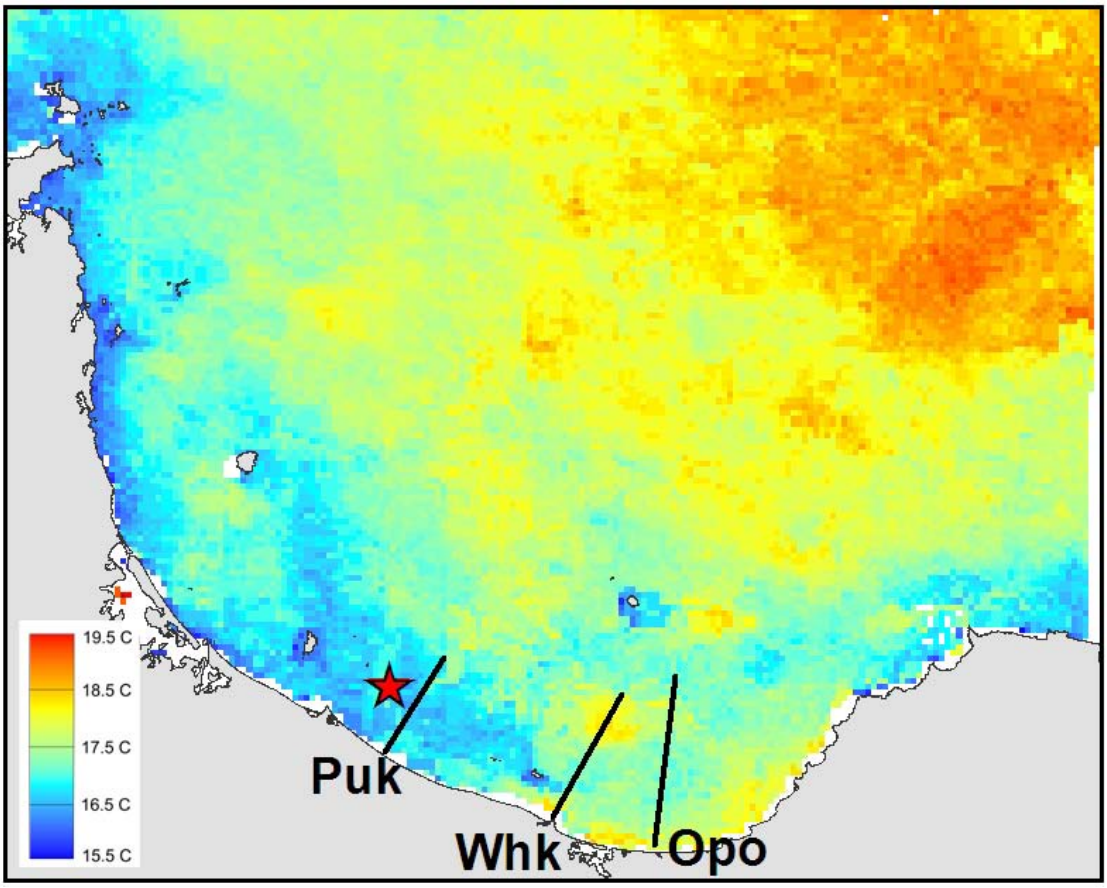

Figure 4.22 AVHRR SSTs within the Bay of Plenty over the period 1 – 3 December 2003, immediately prior to the CTD survey conducted on 3, 4 and 5 December 2003 (Figure 4.25). Locations of CTD transects marked and labelled, Puk = Pukehina, Whk = Whakatane, and Opo = Opotiki. Red star indicates position of ADP.

The two CTD surveys represent different stages in the evolution of an upwelling response within the Bay of Plenty. The later survey (early December) immediately follows a weak upwelling favourable wind stress. A strong water column response is evident near Pukehina with a much weaker signal apparent nearer Whakatane and Opotiki (Figure 4.22). In contrast, the earlier survey (mid October) lagged a strong upwelling favourable wind event by ~14 days and displayed remarkably high sub-surface chlorophyll-a concentrations along with a stronger signal of upwelling at Whakatane and Opotiki than at Pukehina. The predicted (and observed) along-shelf geostrophic current generated by an upwelling favourable wind event is to the SE, along the coast from Pukehina towards Whakatane and Opotiki. Though not evident from these data, it is suggested that the degree of upwelling reduces along the coast towards the NW from Pukehina as a result of the changing coastal and shelf orientation. This would result in a gradual decrease in the proportion of cool, high nutrient water being delivered to the Pukehina site by the along-shelf geostrophic current following the cessation of the upwelling favourable wind stress.

4.7.3 RESOLVING ASSOCIATIONS BETWEEN WIND FORCING, CIRCULATION, AND TEMPERATURES

Lagged cross-correlations were performed between rotated along-shelf wind stress, along and cross-shelf current components (Figure 4.23 and Table 4.6), and time-derivatives of water column temperatures using MATLAB® software. Customisation allowed the use of the full current meter dataset with only the loss of the lag length of data on one side of the gap.

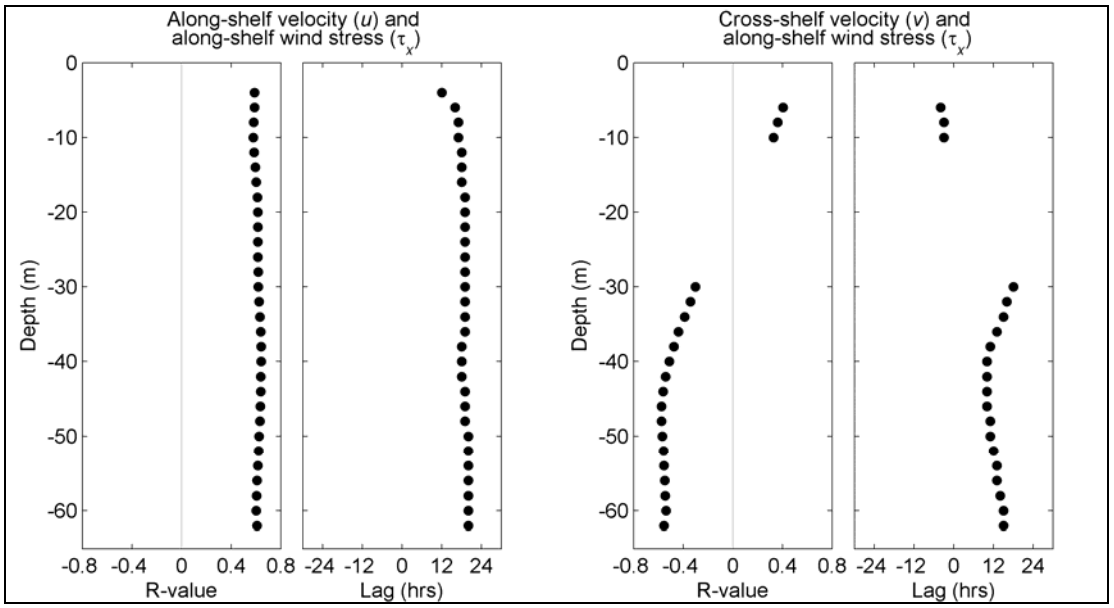

Figure 4.23 Maximum lagged cross-correlation coefficients and associated lag intervals between along-shelf wind stress (τ_x) and low pass filtered along-shelf (*u*) and cross-shelf (*v*) flow components through the water column at the Pukehina 65 m site between 1200 NZST 22 September 2003 and 0700 NZST 2 December 2003 (1699 hr). Non-significant (95% level) correlation coefficients (< 0.3) and associated lag values not plotted (see Allen and Kundu [1978] for determination of significance levels). Positive lags indicate wind stresses leading currents.

Table 4.6 Statistics of mean and low-passed velocity at Pukehina 65 m site for September - December 2003. Insignificant correlations at 95% level marked by *. Record length is 1699hrs

	Along shelf (u, cms^{-1})				Cross-shelf (v, cms^{-1})			
Mid-depth bin (m)	Mean	Std dev	Correlation to τ_x	Lag (hrs)	Mean	Std dev	Correlation to τ_x	Lag (hrs)
4	1.22	11.07	0.59	12	1.15	7.11	0.30*	-3
6	4.08	12.45	0.59	16	0.72	7.55	0.41	-4
8	4.34	12.61	0.58	17	0.66	7.96	0.36	-3
10	4.23	12.19	0.58	17	0.22	7.42	0.33	-3
12	4.01	11.8	0.58	18	-0.11	6.76	0.25	-4
14	3.66	11.47	0.59	18	-0.39	6.28	0.20	48
16	3.22	11.35	0.60	18	-0.57	6.18	0.16*	48
18	2.83	11.29	0.61	19	-0.78	6.04	0.14*	48
20	2.56	11.25	0.62	19	-0.98	5.92	-0.13*	-39
22	2.44	11.25	0.62	19	-1.15	5.82	-0.14*	-39
24	2.31	11.35	0.62	19	-1.25	5.77	-0.18*	19
26	2.19	11.45	0.62	19	-1.31	5.76	-0.21*	19
28	2.11	11.53	0.62	19	-1.31	5.68	-0.25*	18
30	2.04	11.61	0.62	19	-1.33	5.72	-0.30*	18
32	2.05	11.69	0.62	19	-1.31	5.69	-0.34	16
34	2.15	11.81	0.63	19	-1.39	5.67	-0.39	15
36	2.35	12.04	0.64	19	-1.54	5.72	-0.44	13
38	2.65	12.36	0.64	18	-1.71	5.91	-0.48	11
40	2.65	12.62	0.64	18	-1.65	6.15	-0.51	10
42	2.08	12.67	0.64	18	-1.35	6.32	-0.54	10
44	1.51	12.73	0.64	19	-1.16	6.39	-0.56	10
46	1.29	12.79	0.63	19	-1.00	6.62	-0.58	10
48	1.18	12.61	0.63	19	-0.86	6.73	-0.57	11
50	1.05	12.46	0.63	20	-0.76	6.86	-0.57	11
52	0.86	12.25	0.62	20	-0.65	6.96	-0.56	12
54	0.74	11.96	0.61	20	-0.59	7.08	-0.56	13
56	0.56	11.52	0.61	20	-0.55	7.10	-0.55	13
58	0.40	10.97	0.60	20	-0.59	7.08	-0.54	14
60	0.28	10.21	0.60	20	-0.61	6.89	-0.54	15
62	0.22	9.14	0.61	20	-0.61	6.44	-0.56	15
Depth Avg.	2.11	10.19	0.63	19	-0.75	3.10	-0.45	17

Near-surface (<10 m depth) cross-shelf currents (v) are weakly positively correlated with along-shelf wind stress (τ_x), indicating that near-surface currents flow offshore (+v) during wind events from the NW and shoreward (-v) during SE events (Figure 4.23 and Table 4.6). Peak correlations occur with lag intervals of ~ -3 hrs (*i.e.* currents leading wind stress). Short negative lag intervals between near-surface cross-shelf currents and along-shelf wind stress are not uncommon on upwelling shelves (*e.g.* Cushman-Roisin *et al.*, 1983; Dever, 1997; Zeldis *et al.*, 2004a). Deeper (>30 m) cross-shelf currents are negatively correlated to along-shelf wind stress, indicating that deep flows are directed onshore (-v) during NW and offshore (+v) during SE wind conditions. Between 25 and 35% of variability in deep cross-shelf currents can be explained by variability in the along-shelf wind stress (Figure 4.23 and Table 4.6). Peak correlations were found with lag intervals of 12-16 hours (currents following wind stress). The respective near-surface and deep cross-shelf responses to along-shelf winds indicate a horizontal shear layer, in the region of 10-30 m water depth, separating the upper Ekman layer from the lower return flows.

Along-shelf wind stress and along-shelf currents were positively correlated throughout the water column, with peak values occurring at lag intervals of 18-20 hrs (currents following winds). Between 35 and 41% of variability in along-shelf currents throughout the water column can be explained by variability in the along-shelf wind stress (Figure 4.23 and Table 4.6). These results are representative of an along-shelf geostrophic coastal current flowing in the same direction as wind stress and set up by a cross-shelf pressure gradient resulting from the cross-shelf divergence within the upper Ekman layer.

Lag intervals of along-shelf flows throughout the water column and deep cross-shelf flows to along-shelf wind stress (18-20 hrs and ~12–16 hrs respectively) are similar to the local inertial period within the Bay of Plenty (19.6 hrs). While several researchers have used this as evidence in support of a hydrodynamic response to wind forcing (*e.g.* Smith, 1981; Huyer, 1984; McClean-Padman and Padman, 1991; Zeldis *et al.*, 2004a), there is potential that this similarity is more co-incidental and the result of variability in the surface wind stresses (Cushman-Roisen *et al.*, 1983).

Several observational studies have found wind driven currents within upwelling regions (*e.g.* Africa, Peru, Oregon, California) consistent with conceptual models in not only a fluctuating sense but also in the mean (order of one to several months, Allen and Kundu, 1978; Smith, 1981; Dever, 1997). At Pukehina, mean (throughout deployment) across-shelf and along-shelf flows are directed offshore at the surface and shoreward at depth, centred at c.40 m depth (Figure 4.24). Mean along-shelf flows are to the SE, with maximum velocities occurring near the surface and decaying with depth; the mean along-shelf wind stress during the deployment was 0.086 Pa toward the SE (upwelling favourable). Depth averaged along-shelf mean flows are positively correlated to along-shelf wind stress; depth averaged cross-shelf mean flows negatively correlated to along-shelf wind stress, both have strongest correlations in the lower layers (Table 4.6). The lack of volumetric balance in the mean cross-shelf velocity profile (Figure 4.24 and Table 4.6, *i.e.* more water moving onshore than offshore) indicates a positive mean $\delta u/\delta x$ (*i.e.* acceleration of the along-shelf flow) in order to conserve mass. The insensitivity of this imbalance to changes in along-shelf orientation ($\pm 15^{o}$) further indicates that the flow is three-dimensional and does not entirely fit a conceptual two-dimensional model of wind driven upwelling. A similar lack in volumetric cross-shelf balance has been observed within the Oregon upwelling zone (Smith, 1981).

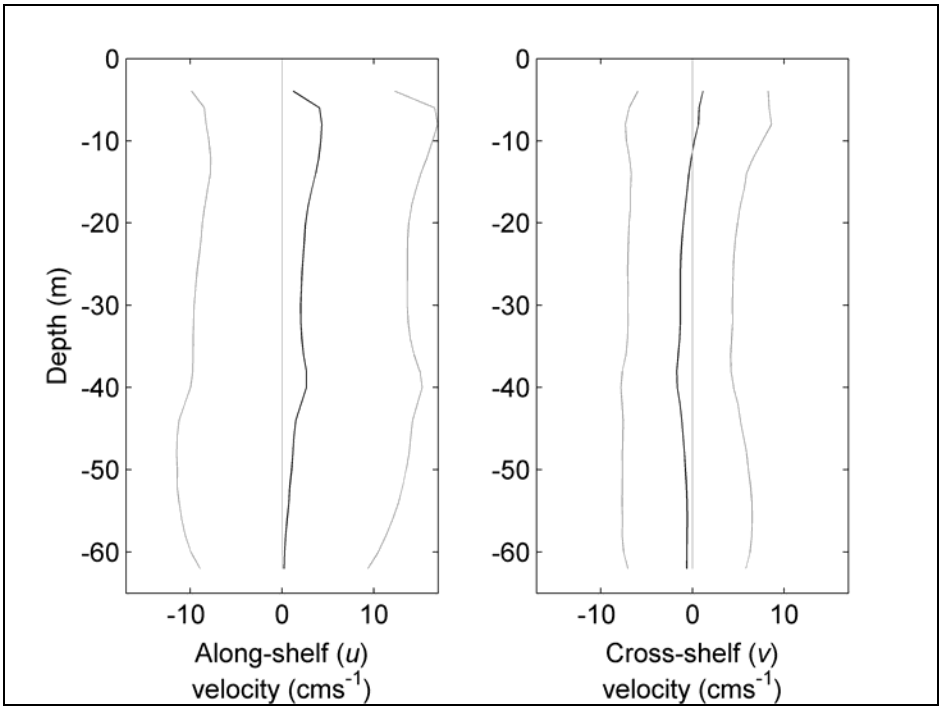

Figure 4.24 Mean along-shelf (u) and cross-shelf (v) currents (heavy lines) between 1200 NZST 22 September 2003 and 0700 NZST 2 December 2003 at the Pukehina 65 m site. Means calculated from hourly time series in 2 m depth bins, light lines are the standard deviations of low pass filtered fluctuations in velocity records.

4.7.3.1 WIND AND CURRENT INFLUENCES ON SUB-SURFACE TEMPERATURES

Temperature structure within shelf waters is dominated by inter-annual variability, the annual cycle, and diurnal heating and cooling within the upper layers. Transient upwelling events occur over timescales ranging from a few days to ~1 month. To provide a first order approximation of potential upwelling induced temperature variability, thermistor data must be filtered to remove both seasonal and shorter diurnal variations (*e.g.* McClean-Padman and Padman, 1991; Chiswell and Schiel, 2001; Roughan and Middleton, 2002). A band-pass butterworth digital filter with half power frequencies corresponding to 2 and 21 days was used to filter the hourly thermistor data (Figure 4.18 d,e).

Time-derivatives of filtered temperature records (2, 8, and 20m depths) display positive correlations with deep (>30 m depth) cross-shelf velocities (Figure 4.25a,b), indicating that when deep cross-shelf velocities are negative (-*v*, *i.e.* onshore and upwelling), the time-derivative of filtered temperature is also negative, indicative of cooling by the upslope movement of cool water. This relationship also suggests a potential warming as a result of deep offshore flows (downwelling). Figure 4.25 shows that the temperature response to deep cross-shelf currents is time staggered through the water column, with lags of 1-2 hrs (20 m temperature), 9-11 hrs (8 m temperature), and 15-20 hrs (2 m temperature). Near-bed temperatures in the outer Hauraki Gulf displayed similar correlations (0.62) and lag times with near-bed cross-shelf velocities (Sharples and Grieg, 1998) as those found at the Pukehina site.

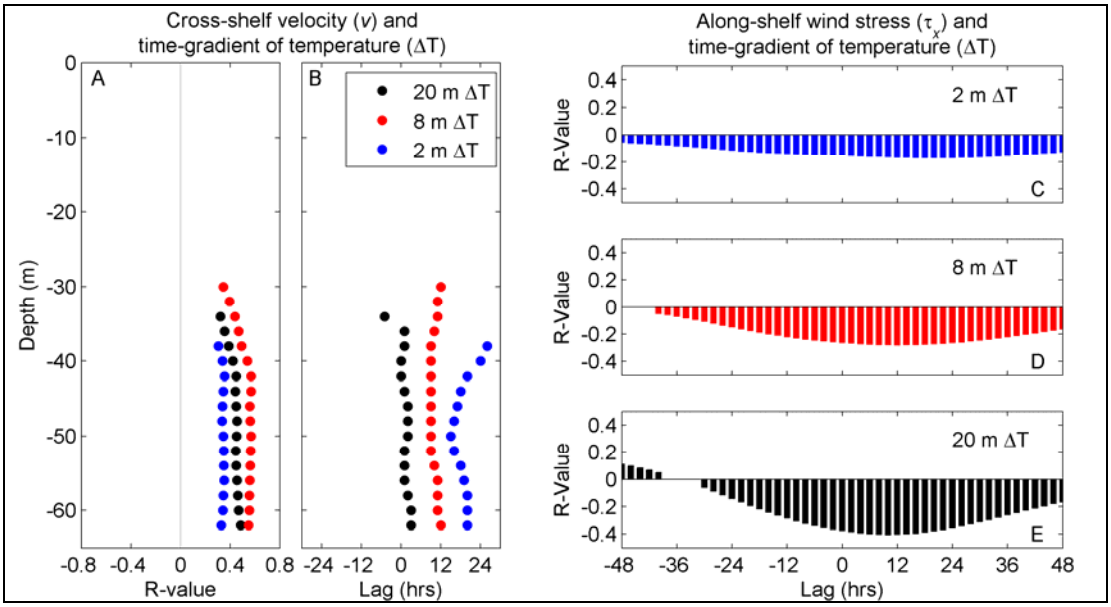

Figure 4.25 Maximum lagged cross-correlation coefficients (a) and associated lag intervals (b) between low pass filtered cross-shelf velocity (*v*) and time-derivatives of band pass filtered ($2 < f < 21$ days) temperature (ΔT) at 2, 8, and 20 m depths. Lagged cross-correlation coefficients between along-shelf wind stress (τ_x) and time-derivative of band pass filtered temperature (c, d, and e). Non-significant (95% level) correlation coefficients not plotted in (a) and (b), in (c), (d) and (e), coefficients less than ~0.3 are non-significant (see Allen and Kundu (1978) for determination of significance levels). Positive lags indicate that time-derivatives of temperature lag cross-shelf velocities (b), and that time-derivatives of temperature lag along-shelf wind stresses (c, d, and e). Data recorded between 1200 NZST 22 September 2003 and 0700 NZST 2 December 2003 at Pukehina 65 m site (1699 hr).

The time-derivative of temperature at 20 m depth is negatively correlated with along-shelf wind stress (Figure 4.25e) with a peak lag of ~12 hours; approximately 12 hours following a positive wind stress event (winds from the NW) the temperature at 20 m decreases. The inverse is true of winds from the SE. Strongest correlations were found at 20 m depth, with no significant relationships nearer to the surface (Figure 4.25c,d,e). The peak temperature response at 20 m depth to the along-shelf wind stress occurs over a shorter time scale than that required to fully develop the upwelling circulation. It is suggested that this is a result of intermediate flows through the central part of the water column (the thermistor at 20 m was located within the intermediate shear layer) and provides some evidence of a three layer upwelling system (*e.g.* Csanday, 1982).

4.7.4 DISCUSSION: UPWELLING DYNAMICS

4.7.4.1 SHELF RESPONSE TO WIND FORCING

Current meter data from Pukehina during spring 2003 indicate that the non-tidal residual circulation within the western Bay of Plenty is highly responsive to wind forcing in both a mean and fluctuating sense. Wind driven Ekman-style dynamics are a significant influence on shelf circulation here.

Strong wind stresses (≥0.3 Pa) from the NW generate along-shelf currents to the SE along with cross-shelf velocities and temperature fluctuations consistent with an

upwelling response. Maximum correlations occur between near-surface cross-shelf velocities and along-shelf wind stress with near zero lag times, indicating that a wind-stress from the NW is accompanied by offshore flows near the water surface. These near surface velocities extend to a depth of ~10-12 m. Approximately one inertial period later, an accompanying shoreward flowing current develops in water deeper than ~30 m. Shortly afterward, an along-shelf current is initiated throughout the water column in the same direction as the wind-stress.

Along-shelf flows transport high-nutrient upwelled water toward locations where the original upwelling response was not as prominent due to the variable orientations of the coast and shelf. Further, following the cessation of upwelling, water 'replacement' at the central upwelling location due to along-shelf flows is nutrient-poor, relative to that upwelled, again due to the variable orientations of the coast and shelf.

The response of the water column at Pukehina during spring is consistent with a three-layer, stratified response to upwelling favourable winds complicated by three-dimensional structure. Near-surface (top layer) cross-shelf velocities respond rapidly to along-shelf wind stress. This response forces the surface layer offshore and lifts the layer beneath up the water column (Csanady, 1982). At Pukehina, this occurs with lag times of order 12 hours, indicated by cross-correlation of the time-derivative of temperature at 20 m depth (middle layer) and along-shelf wind stress. The development of the full upwelling circulation lags the wind stress by ~19 hours, consistent with the local inertial period (though this indeed may be co-incidental, *e.g.* Cushman-Roisin *et al.*, 1983).

Further time is then required for the cool upwelled water to propagate to its maximal distance offshore, which is dependent upon the along-shelf wind stress, upper layer density, upper layer depth, and local Coriolis parameter (Smith, 1981). Based on these parameters within the upper Ekman layer, the time required for the maximal offshore extent of the upwelled water to be reached can be predicted (*e.g.* Csanady, 1981; Roughan and Middleton, 2002; Zeldis *et al.*, 2004a). Application to these data indicate that under the median wind stresses during each upwelling event, predicted times for the plumes to reach their maximal distances offshore are 5 days for the late September event, and 2 days for each of the November events. These predicted values are similar to those observed (Figure 4.18d). These time lags are substantially shorter than that observed by Zeldis *et al.* (2004a) within the Hauraki Gulf, though this can be explained by the reduced distance that the plume travels offshore in the Bay of Plenty (20 km and 10 km) relative to the Hauraki Gulf (40-50 km), and also by the remarkably strong wind stresses during the September event.

Time-derivatives of filtered temperature in the upper-mid water column (2-20 m) are correlated to cross-shelf velocities in the lower layer (>30 m depth) with lag times increasing from the thermocline towards the surface. This can be explained by

assuming a relative uniform vertical velocity throughout the upper-mid water column, resulting from the cross-shelf velocities at depth pushing water up the shelf. The temperature response will be more rapid in areas where the gradient of the temperature profile through depth is greatest (*i.e.* the thermocline). Where the water column temperature profile is more homogenous (*e.g.* the upper 3 m, due to mixing by waves etc) a longer period of upwelling is required to observe a change in temperature due to the circulation. Chiswell and Schiel (2001) found a similar result during upwelling off Kaikoura on New Zealand's South Island using alternative techniques.

Relationships between time-derivatives of filtered temperature and along-shelf wind stress were strongest near the thermocline, with non significant relationships observed at shallower levels, a finding consistent with those of McClean-Padman and Padman (1991), Chiswell and Schiel (2001), and Roughan and Middleton (2002). Huyer (1984), however, found highest correlations in the surface layer in the northern Californian upwelling system, although in that study the data had not been high-pass filtered prior to running the regression analysis and so maintained a strengthening seasonal signal through the upper levels of the water column.

The general results of this study (wind-current cross-correlation profiles, mean flow profiles, wind-current-temperature cross-correlations) are insensitive to small ($\pm 10^{o}$) changes in co-ordinate system orientation.

Similar analyses with current meter records from Opotiki during winter 2004 (Figure 4.21) revealed much weaker correlations. This result is suggestive of a well mixed water column during winter preventing the de-coupling of near-surface and deeper flows to generate Ekman transport. Temperature records indicate a consistently well mixed upper water column at the Opotiki site during winter 2004 (Figure 4.10), in contrast to that of Pukehina during Spring 2003 (Figure 4.9). However, the possibility of a fundamental difference in the forcing of shelf circulation between the Pukehina and Opotiki sites cannot be ruled out due to the differing times of the deployments. From the present data further conclusions regarding differences between these sites cannot be justified.

Though not characterised here, the potential for influences from coastal-trapped waves upon the Bay of Plenty shelf remains a strong possibility given the presence of potential geographic origins such as East Cape and Cook Strait. Though no direct evidence of the presence has yet been published, their presence has been suggested (Bell and Goring, 1996; Stephens *et al.*, 2001). This is explored further in the hydrodynamic modelling chapter (Chapter 5).

4.7.4.2 CROSS-SHELF INTRUSIONS AND DOWNWELLING

Correlations between along-shelf wind stress, cross-shelf currents, and water column temperatures are suggestive of downwelling circulation patterns as a result of downwelling favourable winds (from the SE). While the present dataset is limited in

its ability to resolve responses to strong wind events from the SE, an assessment of historical measurements is advantageous.

Within the outer Hauraki Gulf, where similar wind driven dynamics to those observed at Pukehina have been identified (Zeldis *et al.*, 2004a), a sharp thermal front, located immediately seaward of the shelf edge, with a gradient of >2^{o}C separates cooler coastal waters from the warmer, more saline sub-tropical water being transported by the EAUC (Sharples, 1997). A thermally stratified water column (typical in spring and early summer) along with an absence of upwelling favourable winds (Zeldis *et al.*, 2004a) or even the presence of downwelling favourable winds (Sharples, 1997) leads to the cross-shelf intrusion of sub-tropical waters on to the shelf and near the coast. These cross-shelf intrusions within the outer Hauraki Gulf can have significant consequences as the dominant primary producers in the oligotrophic sub-tropical oceanic water take advantage of the high nutrients in the adjacent coastal water as the two water masses mix during the intrusion events (Sharples, 1997). Whilst the wind driven dynamics of the Pukehina shelf are similar to those of the outer Hauraki Gulf, no such distinct thermal front occurs within the Bay of Plenty. With a more diffuse separation between neritic and oceanic waters (and associated offshore temperature gradients) the hydrographic response of the Bay of Plenty to downwelling favourable wind stresses can be expected to be typically more subtle than that of the outer Hauraki Gulf. An exceptional event (*cf.* Hauraki Gulf) may be required to drive offshore oceanic waters onto the shelf and near the coast within the Bay of Plenty.

One potential event, occurring during the spring-summer of 1992-1993, was spread in spatial extent along New Zealand's north-east coast. Severe disruption was caused to both the shellfish aquaculture industry and to naturally occurring shellfish through the sudden appearance in significant abundances of toxic dinoflagellates (*Alexandruim minutum* and *Gymnodinium* cf. *breve*). The introduction of these dinoflagellates to coastal waters was thought to have been a result of stimulation of existing 'cyst' beds (*A. minutum*) and by an intrusion of offshore waters (*G.* cf. *breve*) (Chang *et al.*, 1996). Though the potential of an intrusion of sub-tropical water was mooted, a lack of research and knowledge surrounding the dynamics of the Bay of Plenty shelf at the time prevented this from being more than an 'expert opinion'.

To test the period surrounding the bloom for wind forcings meteorological data from Tauranga Airport must be used as the QuikSCAT sensor became operational only in 1999. Along-shelf wind velocities at Tauranga Airport correlate well ($R^2 = 0.71$) with those interpolated from the QuikSCAT sensor over a common year of measurement (2003-2004). However, the Tauranga data systematically underestimate the along-shelf wind stress as determined from QuikSCAT data by a factor of 2.2.

Analyses of the Tauranga wind field surrounding the event reveals three periods of wind stress from the SE during October, November and December 1992 (Figure 4.26), followed by persistent upwelling favourable winds during January 1993.

Furthermore, monthly mean along-shelf wind stress during October, November and December 1992 indicate a consistent lack of upwelling favourable NW winds (Figure 4.27), a time when long term monthly means (1993 – 2004, Fig. 11) indicate that these winds are typically at their strongest.

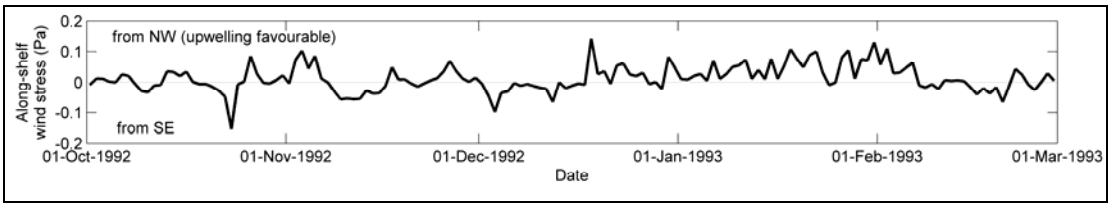

Figure 4.26 Daily mean values of along-shelf wind stress from Tauranga Airport (3 hourly measurements). Along-shelf wind stress at Tauranga underestimates that from QuikSCAT by a factor of 2.2.

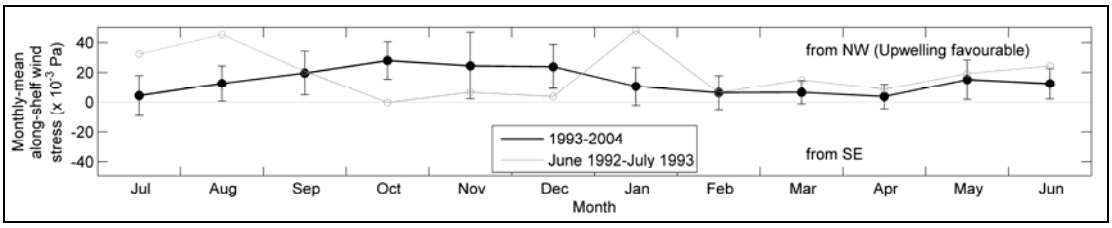

Figure 4.27 Monthly means and standard deviations of along-shelf wind stress measured from Tauranga Airport between 1/1/1993 and 31/12/2004 (black line). Monthly means of along-shelf wind stresses during July 1992 – June 1993 (grey line).

The consistent absence of the normally strong NW winds during October, November, and December (Figure 4.27 and also Bell and Goring, 1998 [see Figure 2.6]), along with the occurrence of three brief, though strong periods of SE winds (Figure 4.26) and the typically thermally stratified water column during spring/summer resulted in a high potential for the encroachment of sub-tropical oceanic water from off the shelf break. Data from Chang *et al.*, (1996) indicate that both surface temperature and salinity at three near-shore sites within the Bay of Plenty were higher during December 1992, than those during either December 1990 or 1991, providing evidence supporting the presence of high temperature, high salinity oceanic water near the coast. Surface temperatures and nutrient profiles in late January 1993 indicated strong upwelling (NO_3-N > 110 μgL^{-1}) in the western Bay of Plenty, near Pukehina (Chang *et al.*, 1996), consistent with both an Ekman-style response to the strong upwelling favourable wind stresses during January 1993 (Figures 4.27 and 4.27), and upwelled nutrient concentrations measured in 2003 (Figure 4.20).

Observational evidence detailing the timeline of the *G.* cf. *breve* bloom from Chang *et al.* (1996) fits well with a hypothesis of wind dominated shelf dynamics. The observed lack of NW winds, periodic short bursts of SE winds, coupled with a thermally stratified water column during October, November and December 1992 acted to transport relatively warm, saline sub-tropical water and its associated phytoplankton species close to the coast. It is unclear, however, whether either of these wind forcings in isolation, or a combination is required to generate the transport. *G.* cf. *breve* concentrations were found to increase strongly seaward (Chang *et al.*,

1996), supporting this proposed offshore source. A change to persistent and strong upwelling favourable winds during January 1993 led to the introduction of large quantities of nutrients to the euphotic zone and was the likely cause of the bloom of the normally nutrient limited *G*. cf. *breve* species. The bloom was observed to persist through January 1993 and decrease steadily from early February (Chang *et al.*, 1996), co-incident with the observed slackening of upwelling favourable winds shutting down the nutrient delivery mechanism (Figures 4.26 and 4.27).

4.8 SUMMARY

SSTs within the Bay of Plenty can be accurately inferred by the AVHRR instrument and do not differ from measured values at the 95% confidence level. Conversely, remotely sensed Case 2 and median filtered Case 2 Chl-a products from the SeaWifS instrument, processed with a locally specific IOP algorithm do a poor job of replicating in-situ point measurements. Observed differences were far greater than those inherent to the sensor (±35%).

The mean annual range of SST over the Bay of Plenty shelf is between 5-7oC, consistent with other shelf locations around New Zealand. A 'tounge' of warm water persists in the nearshore from immediately east of Opotiki to near Te Kaha during the summer months when other near-shore locations display relatively cooler SSTs. Further, the SST data indicates that there is a consistent (spatially and temporally) positive gradient in SST in an offshore direction within the Bay of Plenty. This gradient is stronger and more consistent during winter than that during summer.

Tidally induced water velocities were typically of the order of 2-5 cms^{-1} and 2-10 cms^{-1} at Pukehina and Opotiki respectively, whilst non-tidal residual flows are typically of the order of 20-30 cms^{-1}, indicating that tidal currents form a relatively minor part of the shelf dynamics. Tidally influenced flows are dominated by a combination of M_2, K_1, and O_1 constituents, with the S_2 component being notably weak. No records of internal baroclinic tides in either current meter or thermistor records could be found.

The Bay of Plenty shelf water column is well mixed during winter, with stratification well underway in December, and being broken down again during May. Significant freshwater flows can act to periodically create inverse temperature profiles.

Current meter, thermistor, remotely sensed SSTs, CTD and water sample data indicate that during spring/summer the Bay of Plenty shelf offshore from Pukehina is highly responsive to wind forcing. The response to the wind stress can be observed in both a mean and fluctuating sense. Between 25 and 35% of variability in deep cross-shelf currents, and between 35 and 41% of variability in along-shelf currents throughout the water column can be explained by variability in the along-shelf wind stress. These relationships (magnitude of variability explained and associated lag intervals) are consistent with transient wind driven upwelling and with other locations where this

has been identified in mid-shelf current meter data, *e.g.* the Oregon shelf (Allen and Kundu, 1978; Cushman-Roisin *et al.*, 1983), the northern Californian shelf (Dever, 1997), and the outer Hauraki Gulf, New Zealand (Sharples and Grieg, 1998; Zeldis *et al.*, 2004a). Within the Bay of Plenty, this upwelling acts to reduce nearshore temperatures and provides and important source of new nutrients (100 – 120 μgL^{-1} NO_X-N, 18-20 μgL^{-1} DRP) to the near-shore ecosystem. The spatial extent of these wind driven dynamics is not known (this would require the simultaneous deployment of an array of instruments). However, measurements from Opotiki during winter (well mixed water column) did not display a similar Ekman response to wind forcing.

The relatively large residual variability in the cross-shelf and along-shelf currents remains unexplained, though it is noted that it is likely the result of the interaction of a multitude of complex processes, such as non-local forcing, local wind resonance, small and medium scale topographic influences, wave effects, etc. Supporting the observations of upwelling circulation are the relationships of filtered subsurface temperatures to both deep cross-shelf currents and to along-shelf wind stresses. While the observed relationships suggest a downwelling response to SE winds, a lack of strong wind events from this direction during the deployment, limit conclusive abilities in this regard.

The observed dynamics can be used to explain the cross-shelf intrusion of sub-tropical water leading to a toxic algal bloom within the Bay of Plenty during 1992 and 1993. Any re-occurring similar event would have severe implications for aquaculture developments within the region.